

1 **Repeated mitochondrial capture with limited genomic introgression in a lizard group**

2

3 **Authors:** Wesley J. Read^{1*}, Rebecca J. Laver^{1,2}, Ching Ching Lau¹, Craig Moritz¹, & Stephen M.
4 Zozaya¹

5

6 ¹Division of Ecology and Evolution, Research School of Biology, The Australian National
7 University, Acton, Australian Capital Territory, Australia.

8 ²The University of the Sunshine Coast, Moreton Bay Campus, Petrie, QLD, Australia.

9 *Corresponding author: wesley.read@anu.edu.au

10

11 **Author contributions:** WJR, SMZ, and CM conceived the study; WJR conducted lab work; WJR,
12 CCL, and RJL performed bioinformatics procedures; WJR, SMZ, and CCL performed analyses;
13 WJR and SMZ created figures; WJR drafted the manuscript; all authors contributed to editing the
14 final manuscript.

15

16 **Funding:** This work was funded by Australian Research Council Discovery Projects DP190102395
17 and DP210102267, and an Australian Biological Resources Study NTRGP Postdoctoral
18 Fellowship Grant to SMZ (NTRGI000036).

19

20 **Data Accessibility Statement:** All data and R code available at
21 <https://doi.org/10.6084/m9.figshare.28440584>

22

23 **Conflicts of interest:** The authors declare no conflicts of interest.

24

25 **Ethics approval statement:** Newly acquired samples were collected under Australian National
26 University animal ethics approvals A2019/15 and A2022/07, Western Australia Regulation 25
27 scientific purposes permit FO25000338-3, and NT Parks and Wildlife Commission permit number
28 69132.

29

30

31 **Abstract**

32 Mitochondrial introgression is common among animals and is often first identified through
33 mitonuclear discordance — discrepancies between evolutionary relationships inferred from
34 mitochondrial DNA (mtDNA) and nuclear DNA (nuDNA). Over recent decades, genomic data
35 have also revealed extensive nuclear introgression in many animal groups, with implications for
36 genetic and phenotypic diversity. However, the extent to which mtDNA introgression corresponds
37 to nuDNA introgression varies. Here, we investigated historical and recent introgression in the
38 *Gehyra nana-occidentalis* clade, a complex group of Australian geckos with documented cases
39 of mitonuclear discordance suggestive of repeated mtDNA introgression. We hypothesised that
40 mitonuclear discordance in this clade reflects mtDNA introgression with substantial nuclear
41 introgression. Despite evidence of repeated mtDNA introgression, however, we found little to no
42 evidence of historical nuDNA introgression using exon capture and genome-wide single
43 nucleotide polymorphism (SNP) data. We also found no evidence of gene flow at modern contact
44 zones and detected only a single early generation hybrid. Unsurprising given these results, we
45 found no evidence of transgressive, intermediate, or more variable morphological phenotypes in
46 taxa with introgressed mtDNA. These findings suggest that hybridisation in this system has, at
47 least in some cases, resulted in repeated mitochondrial introgression with little or no nuclear
48 introgression. This pattern aligns with other studies showing limited nuDNA introgression in taxa
49 with mitonuclear discordance, highlighting a potentially broader trend in animal radiations.

50

51 **Keywords:** mitonuclear discordance, contact zone, hybridisation, exon capture, SNP, *Gehyra*

52

53 **Introduction**

54 Hybridisation was once thought to occur rarely in animals (Mayr, 1963), but modern
55 phylogenomics has revealed extensive, post-divergence gene flow across many taxa (Abbott et
56 al., 2013; Mallet et al., 2016). One potential outcome of hybridisation is the exchange of
57 mitochondria between lineages, whereby ‘lineage’ can refer to a genetic lineage within a species
58 or a species itself. This is known as mitochondrial introgression, which is now recognised as
59 common across many taxa (Currat et al., 2008; Toews & Brelsford, 2012). However, the extent to
60 which matching nuclear introgression occurs can vary from extensive (e.g., Sarver et al., 2021; Ji
61 et al., 2023) to limited or absent (e.g., Sloan et al., 2017; Grummer et al., 2018; Mao & Rossiter,
62 2020). Mitonuclear discordance — where evolutionary relationships inferred from mtDNA differ
63 to those inferred from nuDNA — is often the first indication of mtDNA introgression (e.g., Phuong
64 & Moritz, 2017; Pavón-Vásquez et al., 2024). In some cases, mitonuclear discordance may also

65 indicate a homoploid hybrid species, which form instantly via hybridisation; but these appear
66 exceptionally rare (Schumer et al., 2014; Hill, 2019). Species groups showing mitonuclear
67 discordance offer valuable opportunities to examine levels of accompanying nuclear gene flow.

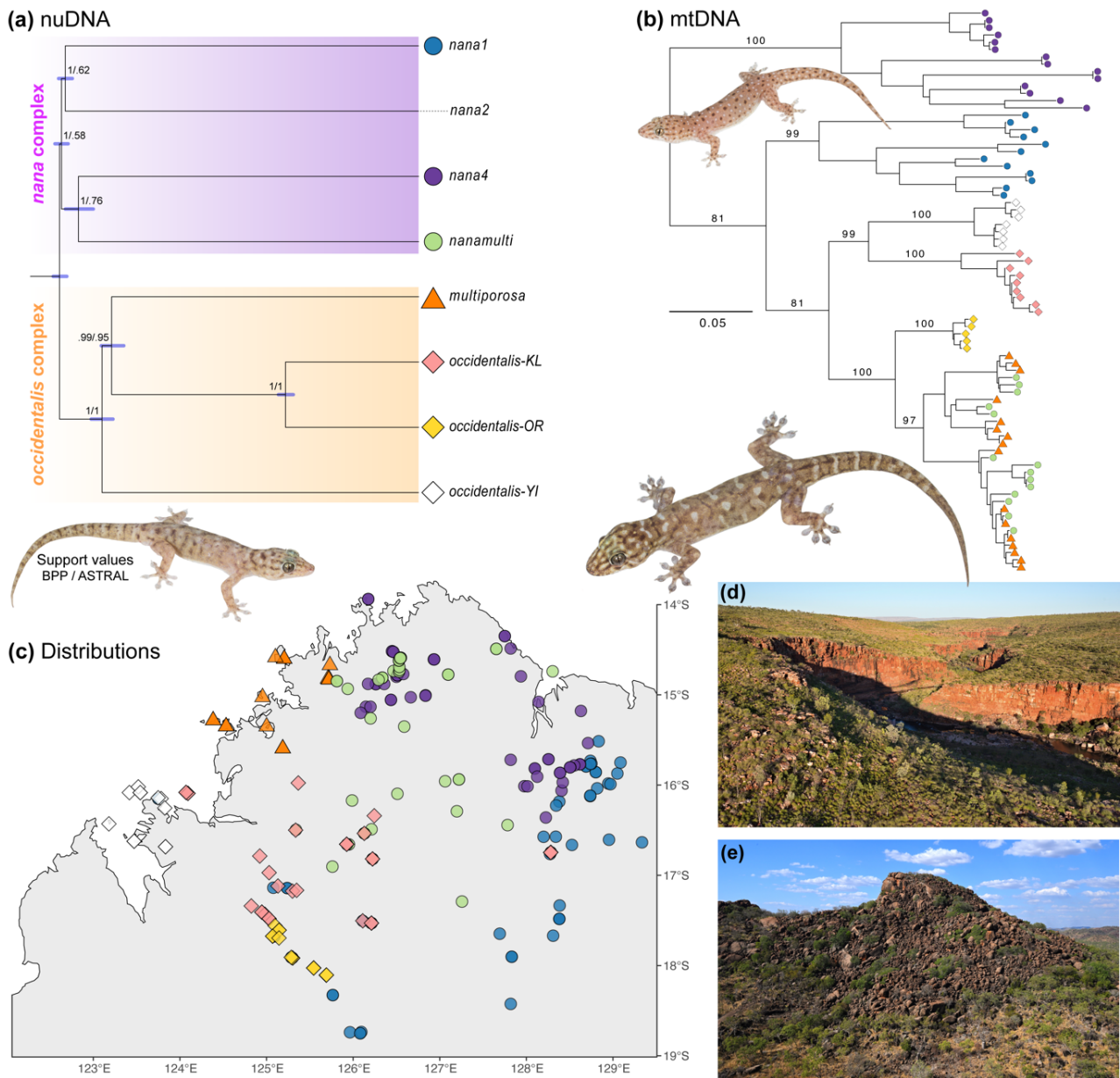
68 Introgression can have significant consequences for lineage divergence and phenotypic
69 variation. If introgression is too frequent it can swamp the genome, potentially reversing the
70 speciation process (Rhymer & Simberloff, 1996). Alternatively, introgression may trigger or
71 facilitate speciation (Edelman & Mallet, 2021) by, for example, introducing adaptive variation
72 (e.g., Staubach et al., 2012) or by altering phenotypes (Lamichhaney et al., 2015; Taylor & Larson,
73 2019 and references therein). Introgressed populations may exhibit novel (transgressive)
74 phenotypes through epistatic interactions or novel allelic combinations (Dittrich-Reed &
75 Fitzpatrick, 2013), or intermediate or more variable phenotypes driven by epistasis or
76 heterozygosity for genes with incomplete dominance (Masello et al., 2019). Transgressive
77 phenotypes are of particular interest in adaptive radiations as access to novel trait space may
78 allow expansion into new niches, thereby facilitating rapid diversification (Wogan et al., 2023).
79 Introgression, therefore, treads a fine line between promoting and inhibiting divergence and,
80 thus, has important implications for understanding diversification (Cruickshank & Hahn, 2014;
81 Harrison & Larson, 2014) and species boundaries (Hillis et al., 2021; Barley et al., 2024).

82 As the mitochondrial genome is effectively a single, non-recombining gene, mitonuclear
83 discordance might not correspond to matching nuDNA introgression. So called 'massive
84 discordance' may occur when a species' native mitochondrial genome is nearly or entirely
85 replaced by mtDNA introgression without matching nuclear introgression (Bonnet et al., 2017).
86 However, determining whether there has been mtDNA introgression based on contrasting mtDNA
87 and nuDNA phylogenies is not straightforward; one must also consider incomplete lineage
88 sorting (ILS) and tree estimation error (Larson et al., 2024). Indeed, identifying introgression in
89 general — whether mtDNA or nuDNA — can be complicated by ILS and the loss of phylogenetic
90 signal through time (Galtier & Daubin, 2008). Model parameter misspecification (Cooper, 2014;
91 Huang et al., 2022) and failure to consider selection (Smith & Hahn, 2024) can also mislead
92 introgression estimates. Establishing confidence in introgression estimates therefore relies on
93 comparing results across different methods of analysis (Hibbins & Hahn, 2022).

94 We explored whether mitonuclear discordance correspond to genomic introgression in a
95 clade of *Gehyra* geckos from the Kimberley region of northern Australia. *Gehyra* is a genus of
96 morphologically conservative geckos with a broad distribution across Australia, Wallacea,
97 Melanesia, and south-east Asia (Heinicke et al., 2011). *Gehyra* diversity is highest in Australia,
98 with 50 recognised species (Wilson & Swan, 2020; Uetz et al., 2024) comprising two broad clades

99 of Plio-Miocene origin: the typically small-bodied *punctata-variegata* group (Ashman et al., 2019),
100 and the large-bodied *australis* group (Sistrom et al., 2009; Oliver et al., 2020). Several unresolved
101 species complexes remain within the *punctata-variegata* group, including the *Gehyra nana* and
102 *G. occidentalis* complexes of the Kimberley region (Oliver et al., 2016; Doughty et al., 2018; Lau
103 et al., 2024), which we hereafter refer to as the *nana-occidentalis* clade. Phylogenetic analyses of
104 the *nana-occidentalis* clade, using geographically dense sampling of mtDNA and exon capture
105 sequencing, have identified eight lineages within this group (Figure 1; Oliver et al., 2016; Moritz et
106 al., 2018; Lau et al., 2024): *nana1*, *nana2*, *nana4*, and *nanamulti* in the *G. nana* complex;
107 *occidentalis-KL*, *occidentalis-OR*, *occidentalis-YI*, and *G. multiporosa* (simply '*multiporosa*'
108 hereafter) in the *G. occidentalis* complex. Lineages within each of the two complexes are
109 morphologically similar and typically replace each other at parapatric boundaries, although
110 *nana4* and *nanamulti* occur in mosaic sympatry. In contrast, members of the smaller-bodied
111 *nana* complex often co-occur with members of the *occidentalis* complex. Of particular interest in
112 this clade is the strong evidence of mitonuclear discordance. One example is the *nanamulti*
113 lineage that — while nested within the *nana* complex for nuDNA — has mtDNA that is
114 interdigitated within *multiporosa* (Moritz et al., 2018; Figure 1), suggesting repeated mtDNA
115 introgression between these distantly-related lineages, rather than simple estimation error or ILS.
116 The sympatry with *nana4* and massive introgression for mtDNA suggests the hypothesis that
117 *nanamulti* itself possibly arose via homoploid hybrid speciation. Further mitonuclear
118 discordance is observed among lineages in the *occidentalis* complex (Figure 1; Oliver et al.,
119 2016; Moritz et al., 2018; Lau et al., 2024), although here evidence of mtDNA introgression, rather
120 than ILS, is less clear as each lineage is reciprocally monophyletic and phylogenetically within
121 the same species complex (unlike *nanamulti* and *multiporosa*). Given such complex mitonuclear
122 discordance, this group offers a good opportunity to investigate whether mitonuclear
123 discordance corresponds to substantial nuclear introgression.

124 Here, we used exon capture and genome-wide SNP data to test for both historical and
125 recent genomic introgression in the *nana-occidentalis* clade. We first performed hypothesis-
126 based tests of historical introgression informed by cases of mitonuclear discordance, the results
127 of which we then corroborated using D-statistics. We then assessed recent or ongoing
128 introgression at two modern contact zones that include lineages with evidence of mitonuclear
129 discordance. Finally, we assessed whether lineages with introgressed mtDNA exhibit
130 transgressive, intermediate, or more variable phenotypes.



131

132

133

134

135

136

137

138

139

140

141

142

143

144

FIGURE 1. Relationships and distributions of the *Gehyra nana-occidentalis* clade. (a) Species tree inferred from 1000 nuDNA exons using BPP, with support shown for both BPP and ASTRAL (identical topologies). Note that *nana2* is included here but not elsewhere as it occurs outside the focal Kimberley region. (b) MtDNA relationships among focal lineages inferred with IQ-TREE, showing several cases of discordance with respect to nuDNA ancestry. Ultrafast bootstrap support values are shown for major branches. (c) Lineage distributions in Australia's Kimberley region based on samples with nuDNA data. (d–e) Typical habitat, showing sandstone gorges (d) and granite boulders (e). Gecko photos show *occidentalis-OR* (left), *nana4* (top-right), and *occidentalis-KL* (bottom-right). Photos: Ian Bool (d,e); Scott Macor (geckos).

145 **Methods**

146 Exon capture sequence data

147 We obtained published nuDNA exon capture sequence data spanning > 1000 loci to perform
148 phylogenetic network analyses. Sequence data were acquired from Moritz et al. (2018) and Lau
149 et al. (2024) for the following *Gehyra* species/lineages: *nana1*, *nana2*, *nana4*, *nanamulti*,
150 *multiporosa*, *occidentalis*-KL, *occidentalis*-OR, and *occidentalis*-YI, with *G. paranana* used as the
151 outgroup. These included 71 samples with 4–14 samples per focal lineage and a single sample of
152 *G. paranana* (Table S1). Briefly, these data were produced using the targeted exon capture
153 approach described in Moritz et al. (2018). Sequences were processed, filtered, and aligned
154 using the EAPhy pipeline (Blom, 2015). Loci with ≥ 11 missing individuals were removed, yielding
155 a dataset of 1,478 exonic loci. Alignments were manually inspected prior to subsequent analysis
156 to ensure correct reading frames, with no missense mutations or unexpected stop codons within
157 the respective exons.

158

159 Reduced-representation genomic sequence data

160 Genome-wide reduced-representation sequencing was done to obtain genome-scale SNP data
161 to test historical introgression using *D*-statistics and to perform contact zone analyses. We used
162 DArTseq via Diversity Arrays Technology (DArT; Canberra, Australia), which involves genome
163 fragmentation with two restriction enzymes (PstI/HpaII) followed by filtering based on fragment
164 size and subsequent Illumina short-read sequencing (Sansaloni et al., 2010; Kilian et al., 2012),
165 yielding thousands of 60–80 bp sequence fragments. SNP calling and associated filtering is then
166 done across all samples via DArT's proprietary pipeline. Newly generated DArTseq data ($n = 35$)
167 were combined with data for relevant lineages from Fenker et al. (2021) and Lau et al. (2024). Our
168 final dataset included 242 individuals sampled across lineage ranges and contact zones, and
169 including *G. paranana* as an outgroup (Table S2). DNA was extracted for newly sequenced
170 samples using a Qiagen DNeasy Blood & Tissue Kit.

171 SNP data were filtered separately for each analysis to maximise the number of variant
172 sites for each data subset. We used *dartR* v.2.9.7 (Gruber et al., 2018) to filter data in the
173 following order: minimum read depth ≥ 6 ; maximum read depth ≤ 80 ; reproducibility ≥ 0.99 ; call
174 rate by locus ≥ 0.8 ; call rate by individual ≥ 0.5 ; minor allele count ≥ 3 (to ensure a given allele is
175 present in at least two individuals); removal of monomorphic loci; retain only one variant site per
176 locus (using method = "best" to retain the site with the highest PIC score). The final dataset of
177 samples across all focal lineages contained 3,966 variant sites. Before continuing, we used the
178 *gl.pcoa()* function in *dartR* to perform a Principal Coordinates Analysis (PCoA) on these data to

179 confirm the lineage assignment of newly sequenced samples (Figure S1). After filtering, a total of
180 1,828 variant sites were retained for the *multiporosa*/nanamulti contact zone, and 2,192 variant
181 sites were retained for the nanamulti/nana4 contact zone.

182

183 mtDNA data and phylogenetics

184 Phylogenetic analysis of mtDNA sequence data was done to illustrate the mitonuclear
185 discordance demonstrated in previous studies. For relevant lineages, we obtained sequence
186 data for the 1,038 bp *NADH dehydrogenase subunit 2 (ND2)* locus from previous studies
187 (Doughty et al., 2012; Oliver et al., 2017; Moritz et al., 2018; n = 468). We then generated new *ND2*
188 sequences for those samples with genomic data but lacking mtDNA data (n = 132) using the
189 MinION barcoding method from Srivathsan et al. (2021). Methods followed those presented in
190 Zozaya et al. (2024) except using the primers M112F (5'- AAGCTTTCGGGGCCCATAACC -3') and
191 M1123R (5'- GCTTAATTAAGTGTYTGAGTTGC -3') from Sstrom et al. (2009). The resulting *ND2*
192 sequences were aligned with those obtained from previous studies using MAFFT in Geneious
193 Prime v. 2021.2.2, which yielded a final alignment of 1,038 bp across 600 samples, including one
194 *G. spheniscus* as the outgroup (Moritz et al. 2018). The alignment was inspected for gaps,
195 unexpected stop codons, or frame shifts, followed by phylogenetic analysis using IQ-TREE v.
196 2.2.0 (Minh et al., 2020). The alignment was partitioned by codon position, with ModelFinder
197 (Kalyaanamoorthy et al., 2017) used to determine the best partition scheme and substitution
198 model, and statistical support determined with 1000 ultrafast bootstrap (UFB) replicates (Hoang
199 et al., 2018). The final partition and model scheme was: 1st position (TIM+F+I+G4); 2nd position
200 (TVM+F+G4); 3rd position (GTR+F+I+G4). We also re-ran this analysis with a subset of 78 samples
201 to better visualise mtDNA relationships with fewer samples.

202

203 NuDNA phylogenomics

204 Our analyses of historical introgression depend on accurate knowledge of phylogenetic
205 relationships. Given the varying phylogenetic relationships inferred for the *nana-occidentalis*
206 clade, including variable support for the monophyly of lineages of *G. nana* itself in previous
207 studies (Moritz et al., 2018; Ashman et al., 2018; Lau et al., 2024), we performed several
208 phylogenomic analyses using exon capture sequence data to better understand relationships
209 among the *nana-occidentalis* clade. Although it occurs outside our study area, we included the
210 Northern Territory *nana2* lineage in all phylogenomic analyses to test the monophyly of *G. nana*.
211 All phylogenomic analyses used the exon capture dataset. We first performed maximum
212 likelihood (ML) phylogenetic analysis on the concatenated 1,478 exon alignment using IQ-TREE

213 v2.2.2.6 (Minh et al., 2020) to confirm lineage assignment for all samples. The analysis was
214 partitioned by locus with modelfinder (Lanfear et al., 2012; Kalyaanamoorthy et al., 2017) used to
215 determine the best partition scheme (MFP+merge) and substitution models. We specified 1000
216 UFB replicates implemented via ufboot2 (Hoang et al., 2018) in addition to branch support
217 metrics via a Shimodaira–Hasegawa-like approximate likelihood ratio test (SH-aLRT; Guindon et
218 al., 2010; Hoang et al., 2018) with 1000 replicates. We used genesite resampling to resample
219 partitions and sites within partitions (Gadagkar et al., 2005; Seo et al., 2005). Next, we performed
220 species tree analysis using the quartet-based algorithm implemented in ASTRAL-III v5.7.8
221 (Rabiee et al., 2019). ASTRAL requires gene trees as input, which were estimated for each of the
222 1,478 exons using IQ-TREE v2.2.2.6, with modelfinder used to determine the best substitution
223 model for each locus, with 1000 UFB replicates. Prior to ASTRAL analysis, gene tree branches
224 with bootstrap support < 30 were collapsed using TreeCollapserCL4 (Hodcroft, 2016) to improve
225 species tree accuracy and branch support (Simmons & Gatesy, 2021). Finally, we used BPP v4.7
226 (Flouri et al., 2018) to perform Bayesian multispecies coalescent phylogenetic analysis. We used
227 the 1000 longest exons (108–2,088 bp; median = 228 bp) with a maximum of seven missing
228 individuals, using 3–4 individuals with the least missing data from each lineage, and with one *G.*
229 *paranana* sample included as an outgroup. Only three samples were included from *multiporosa*
230 and *occidentalis*-YI due to the remainder missing large amounts of sequence data (> 30%). The
231 analysis was initially run as an A01, specifying the guide tree topology as inferred by ASTRAL-III.
232 We assigned diffuse inverse-gamma priors for population size $\theta \sim \text{InvGamma}(3, 0.003)$ and tree
233 height $\tau \sim \text{InvGamma}(3, 0.003)$. We ran the MCMC for 1,000,000 iterations after a burn-in of
234 100,000 iterations, with sampling every two iterations for a total of 500,000 samples.

235 236 Testing historical introgression using network analysis

237 We conducted hypothesis-based tests of introgression using the multi-species-coalescence-
238 with-introgression (MSCi) phylogenetic network analysis in BPP v.4.4.0 (Flouri et al., 2020) to
239 specifically test for genomic introgression in cases where there is evidence of mitonuclear
240 discordance (Figure 1). Specifically, we tested for introgression between: i) *multiporosa* and
241 *nanamulti*; ii) *multiporosa* and *occidentalis*-OR; and iii) *occidentalis*-YI and *occidentalis*-KL.
242 There is clear evidence of repeated mtDNA introgression from *multiporosa* to *nanamulti*, whereas
243 there are two equivocal scenarios of mtDNA introgression within the *occidentalis* complex (see
244 Results). BPP makes full use of the sequence data under the MSC, produces robust inferences
245 even under model miss-specification (Huang et al., 2022), and is computationally efficient.
246 Analyses used subsets of the same 1,000 loci used for the phylogenomic analysis above. As BPP

247 requires a user-specified phylogeny, analyses were run with three tips to avoid the uncertain
248 phylogenetic relationships and reduce computational burden. Three tips were used, rather than
249 two, because the MSCi cannot estimate introgression when the lineages involved are sisters
250 (Hibbins & Hahn, 2022). The following relationships were specified for each combination of
251 lineages: i) (*multiporosa*, (nanamulti, *nana4*)); ii) (*multiporosa*, (*occidentalis*-OR, *occidentalis*-
252 KL)); iii) (*occidentalis*-YI, (*occidentalis*-KL, *occidentalis*-OR)). Each tip included 3–4 of the most
253 data complete samples; only three each of *multiporosa* and *occidentalis*-YI were used due to
254 excessive missing data in the remaining samples. Three introgression scenarios — two
255 unidirectional models and one bidirectional model — were run for each of these lineage
256 combinations. For example, unidirectional introgression was tested from *multiporosa* to
257 nanamulti and then from nanamulti to *multiporosa*, each as a separate analysis, and then a
258 model was run with bidirectional introgression between the two lineages. Priors for population
259 size (θ) and tree height (τ) were both assigned as InvGamma(3, 0.003), while the prior for
260 introgression probability (φ) was assigned as Beta(2, 4). Each analysis was run for 1,000,000
261 iterations after a burn-in of 100,000 iterations, sampling every two iterations, for a total of
262 500,000 sampled iterations. All analyses were executed twice to check for convergent results,
263 and posterior distributions were checked using TRACER v.1.7.2 (Rambaut et al., 2018). We
264 assessed the statistical significance for each model by calculating Bayes factors (B_{10}) via the
265 Savage-Dickey density ratio (Dickey, 1971), which uses the MCMC sample to assess whether the
266 posterior distribution of φ differs from what would be expected given the priors, with $B_{10} \geq 20$
267 indicating a strongly supported introgression event (Ji et al., 2023).

268

269 Tests for historical introgression using D statistics

270 We used the genome-wide SNP dataset to estimate D - and f -branch statistics using *Dsuite*
271 (Malinsky et al., 2021). This method assesses all lineage combinations for introgression, except
272 sister lineages, and then accounts for correlated allele frequencies among tips to identify
273 introgression events on the internal branches of the tree (Durand et al., 2011; Patterson et al.,
274 2012). We specified the topology recovered by both ASTRAL and BPP, again using *G. paranana* as
275 the outgroup. P-values were calculated using the jack-knife method and, as more than three
276 lineages were assessed, we applied the False Discovery Rate (FDR) correction to account for
277 false positives due to multiple pairwise comparisons (Benjamini & Hochberg, 1995) using the
278 ‘p.adjust’ function as suggested by Malinsky et al. (2021).

279

280

281 Contact zone analyses

282 We analysed two contact zones, one between *multiporosa* and *nanamulti*, and another between
283 *nana4* and *nanamulti*. All analyses described below were run separately for each of these two
284 contact zones, and SNP filtering (see above) was done separately for each to maximise the
285 number of variant sites. We first used NewHybrids (Anderson & Thompson, 2002) to test whether
286 any individuals were F1, F2, or first-generation backcross (BC1) hybrids. This was done with the
287 SNP dataset via the *gl.nhybrids()* in *dartR* using the 'AvgPIC' method, 100 sweeps, and a burn-in of
288 100. Next, we estimated the optimal number of ancestral populations (K) and individual
289 admixture proportions using sNMF (Frichot et al., 2014) via the R package *LEA* (Frichot & Rançois,
290 2015). Genotypic clustering analyses can under- or over-estimate the optimal K value, and thus
291 admixture estimates, when there is strong population structure and sparse or uneven sampling
292 (Puechmaille, 2016; Lawson et al., 2018; Wang, 2022). To mitigate the influence of within-lineage
293 population structure, we excluded samples outside a 40–80 km radius (depending on the
294 lineages included and sampling density; Table S3) centred on each contact zone. Each analysis
295 was run with K = 1–5, alpha = 100, 100 repetitions, and masking = 0.05. We considered the
296 optimal K value to be the one that produced the lowest average cross entropy (ce) score. Given
297 the biases mentioned above, we verified both the K and admixture estimates using isolation-by-
298 distance (IBD) plots (e.g., Prates et al., 2023; Zozaya et al., 2024), which plot pairwise geographic
299 distance against pairwise F_{ST} (Wright, 1943; Weir & Cockerham, 1984; Weir & Hill, 2002) among
300 individuals at each contact zone. Pairwise geographic distances (km) were calculated using the
301 *earth.dist()* function in *fossil* v0.4.0 (Vavrek, 2011) and pairwise F_{ST} was calculated using the
302 *calculate.all.pairwise.fst()* function in *BEDASSLE* v1.6.1 (Bradburd et al., 2013). If there is no
303 introgression at a given contact zone we expect between-lineage pairwise F_{ST} to be relatively high
304 and unrelated to the geographic distances among samples, whereas if there is recent or ongoing
305 introgression we expect between-lineage pairwise F_{ST} to decrease as geographic distances
306 decrease. Finally, for each contact zone we performed a PCoA using the *gl.pcoa()* function in
307 *dartR* to further verify the optimal K value and visualise the major axes of genetic variation.

308

309 Morphometric analyses

310 Morphological data for relevant lineages were collected from genotyped specimens at the
311 Western Australian Museum (WAM; Table S4). We measured 10 linear traits (illustrated in Figure
312 S2) to the nearest 0.1 mm using Mitutoyo digital callipers: snout-to-vent length (SVL); head length
313 (HL); snout length (SL); head width (HW); head depth (HD); orbit width (OR); width-between-eyes
314 (WBE); inter-limb-length (ILL); hindlimb-length (HLL); and forelimb-length (FLL). Sample sizes for

315 each lineage are: *multiporosa* = 16; *occidentalis*-KL = 45; *occidentalis*-YI = 12; *occidentalis*-OR =
316 5; *nanamulti* = 37; *nana4* = 43; *nana1* = 22.

317 Using these data, we first tested for sexual dimorphism via a permutational multivariate
318 analysis of variance (PerMANOVA) using the R package *RRPP* (Collyer et al., 2015). Sexual
319 dimorphism was tested using three lineages for which we had the largest sample sizes
320 (*occidentalis*-KL, n = 44; *nana1*, n = 42; and *nana4*, n = 22). All traits were log transformed prior to
321 analysis. We used the *lm.rrpp()* function with the 10 log-transformed morphological traits as
322 dependent variables and lineage, sex, and their interaction as predictor variables with 10,000
323 permutations and as a type III MANOVA for significance testing. The effect of sex was not
324 significant ($df = 1/103$, $F = 2.976$, $Z = 1.532$, $R^2 = 0.006$, $P = 0.064$; Table S5) and was not
325 considered in subsequent analyses. We then tested for morphological divergence among
326 lineages. A PerMANOVA was performed using the 10 log-transformed traits as dependent
327 variables with lineage as the predictor variable and 10,000 permutations for significance testing.
328 We then ran pairwise contrasts using the *pairwise()* function for each lineage pair, followed by P-
329 value adjustment using the *p.adjust()* function to account for inflated type 1 error with the FDR
330 method (Benjamini & Hochberg, 1995). We visualised morphological variation and divergence,
331 and identified traits associated with the greatest axes of variation, via a Principal Components
332 Analysis (PCA) using the *rda()* function (scale = T) in the R package *vegan* (Dixon, 2003). Finally,
333 we tested whether intraspecific phenotypic variation differed among lineages, which could
334 reflect increased genetic variation due to introgression. We conducted a Fligner-Killeen test
335 (Fligner & Killeen, 1976), a non-parametric test that compares variances among multiple groups,
336 even when the assumption of normality is violated, in this case by potential outliers of
337 exceptionally large or small size. This is a univariate test and, as previous studies have
338 established body size as the primary trait of variance in *Gehyra* (Sistrom et al., 2012; Ashman et
339 al. 2019; Moritz et al., 2018), we assessed phenotypic variance using log-transformed SVL as a
340 proxy for body size across all lineages.

341

342 **Results**

343 *NuDNA phylogenomics*

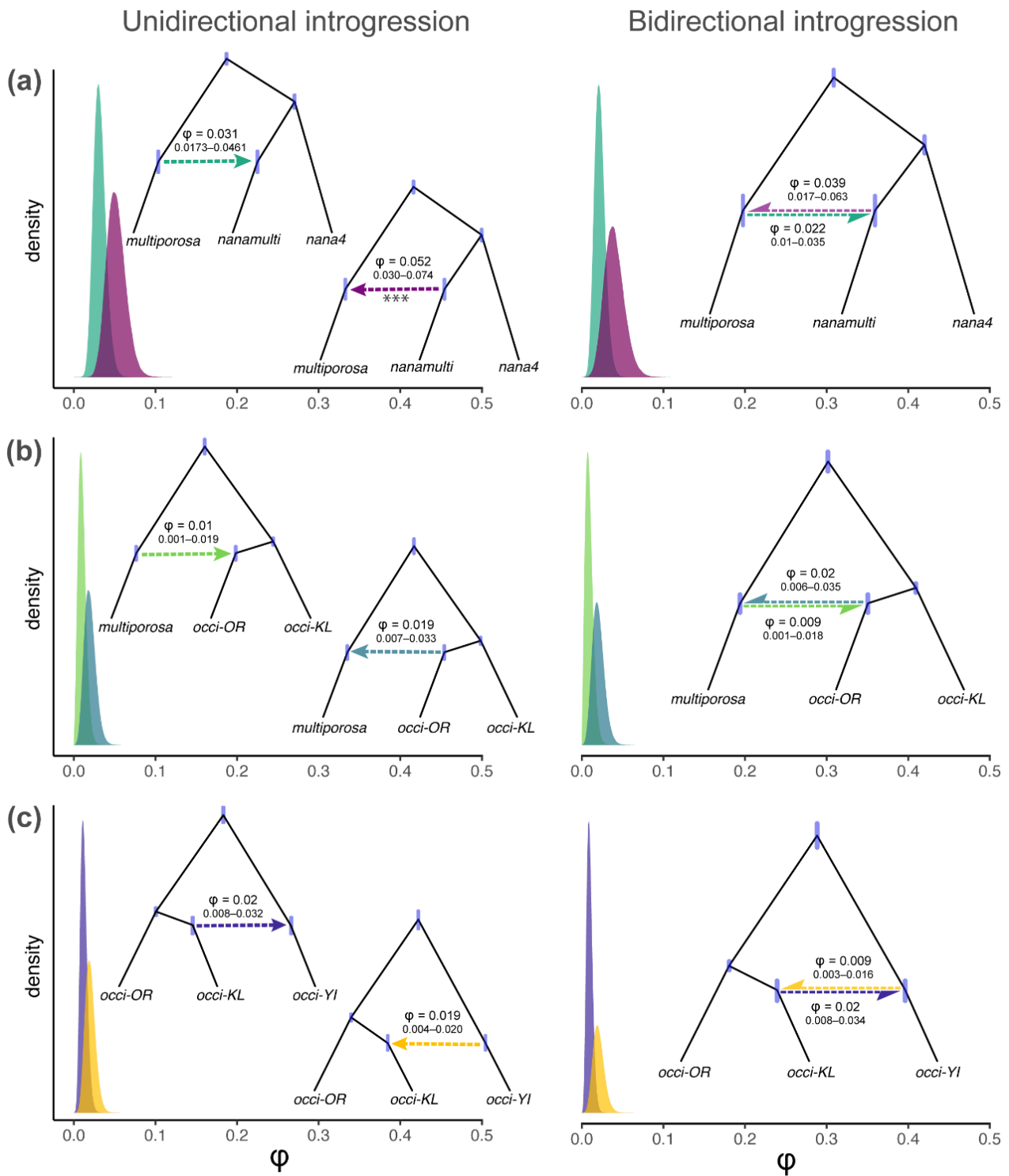
344 All eight previously identified lineages were each recovered as monophyletic clades with strong
345 support (IQ-TREE: UFB = 100; ASTRAL: pp \geq 0.99 for all; Figures S3, S4). All three phylogenomic
346 analyses recovered the *occidentalis* complex as a monophyletic clade with full support (Figures
347 1a, S3, S4), with *occidentalis*-YI being the deepest branching lineage, followed by *multiporosa*,
348 and *occidentalis*-KL and *occidentalis*-OR as sister lineages. Relationships among the four

349 lineages of the *nana* complex, however, differed between the concatenated and species tree
350 approaches (Figures 1a, S3, S4). The concatenated IQ-TREE analysis placed *nana4* as sister to
351 the remaining *nana-occidentalis* clade, reducing the "*nana* complex" to *nana1*, *nana2*, and
352 *nanamulti*, with *nana2* recovered as the first-branching lineage in this group (UFB = 75, aLRT =
353 87). In contrast, the *nana* group was recovered as monophyletic with low support in the ASTRAL
354 analysis (pp = 0.58) and high support in the BPP (pp = 1) analysis. Both species tree analyses
355 recovered *nana4* + *nanamulti* and *nana2* + *nana1* as sister pairs, although ASTRAL inferred this
356 with low support (pp = 0.76 for *nana4* + *nanamulti*; pp = 0.62 for *nana2* + *nana1*) compared to BPP
357 (pp = 1 for both sister pairs). With respect to the *nana* complex, these relationships are
358 consistent with the 100 locus StarBEAST2 phylogeny from Moritz et al. (2018). Notably, low
359 support for relationships within the *nana* complex are associated with very short internode
360 lengths in the species tree analyses. What is important for our introgression analyses below —
361 which require phylogenetic relationships to be pre-specified — is that the species tree methods
362 each recover *nana4* and *nanamulti* as sister lineages.

363

364 MtDNA phylogenetics

365 Five of the seven focal lineages are recovered as monophyletic mtDNA clades (Figures 1b, S5),
366 while individuals of *nanamulti* are extensively interdigitated among *multiporosa*, often with very
367 short branch lengths between samples of different nuDNA ancestry. All individuals assigned to
368 *nanamulti* by nuDNA SNP analyses (Figure S1) have *multiporosa* mtDNA and are distributed
369 across multiple, well-supported mtDNA clades within *multiporosa*. From these observations, we
370 infer recent and repeated mtDNA introgression from *multiporosa* to *nanamulti*. *Gehyra*
371 *occidentalis*-OR is recovered as sister to *multiporosa*/*nanamulti* with respect to mtDNA, despite
372 *occidentalis*-OR having a close sister relationship with *occidentalis*-KL based on nuDNA.
373 Furthermore, *occidentalis*-KL and *occidentalis*-YI are most closely related with respect to mtDNA
374 despite *occidentalis*-YI being the first-branching lineage in the nuDNA phylogenies. These results
375 suggest two possible cases of historical mtDNA introgression in the *occidentalis* complex – either
376 from *occidentalis*-YI to *occidentalis*-KL resulting in their mtDNA clades being most closely
377 related, or from *multiporosa* to *occidentalis*-OR leading to close relationships of their mtDNA
378 lineages.



379

380 **Figure 2.** Results of hypothesis-based tests of introgression using the MSCi model implemented
 381 in BPP. Each row (a–c) shows a different combination of lineages. The left column shows results
 382 for unidirectional models; the right column shows results for the corresponding bidirectional
 383 model. Trees within panels show the scenarios being tested, with coloured arrows matching the
 384 posterior distributions within the respective panel. Values show means and 95% credible
 385 intervals for introgression probability (ϕ). Only the unidirectional model from nanamulti to
 386 *multiporosa* (***) was strongly supported ($B_{10} \geq 20$; Table 1).

387

388 Historical introgression

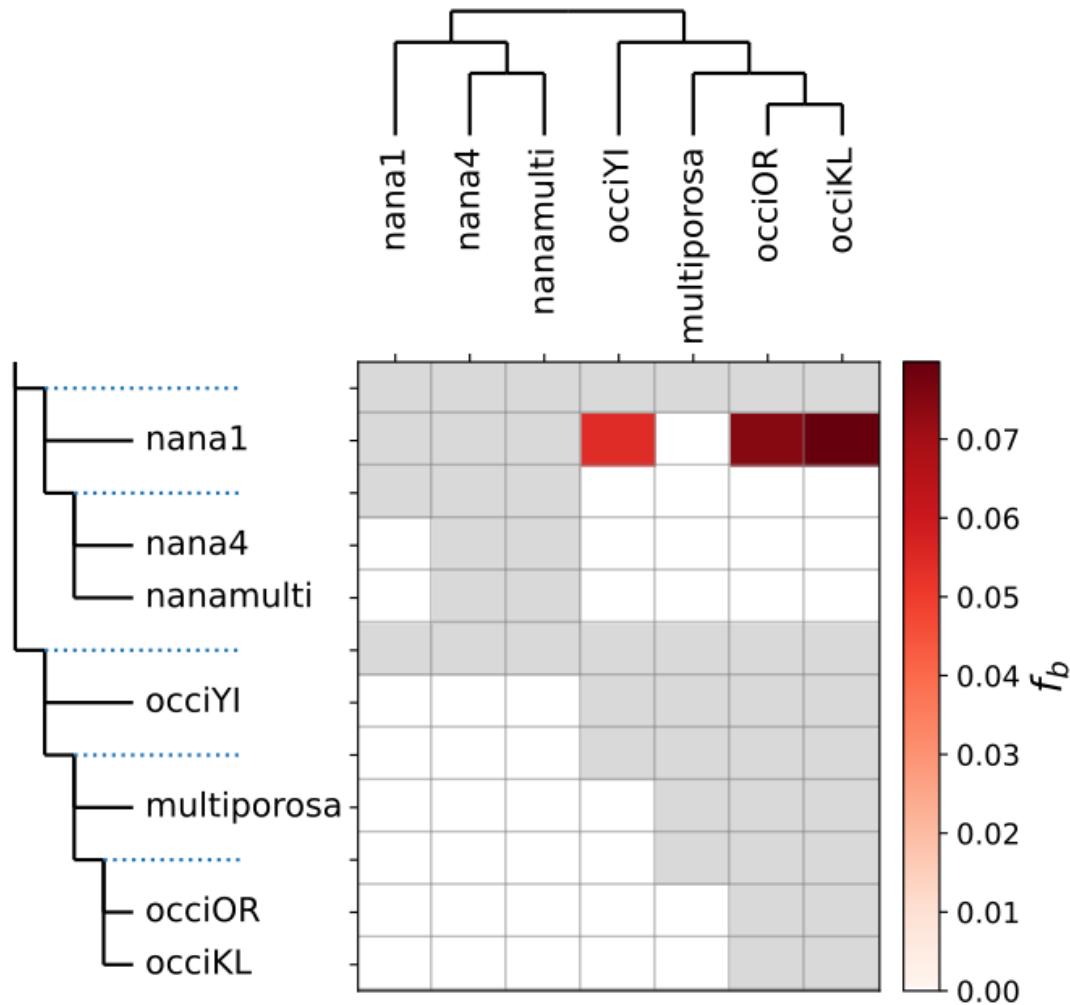
389 We used the MSCi in BPP to test introgression scenarios between *multiporosa* and *nanamulti*,
 390 *multiporosa* and *occidentalis-OR*, and *occidentalis-YI* and *occidentalis-KL*. Introgression was
 391 strongly supported ($B_{10} \geq 20$) only for unidirectional introgression from *nanamulti* to *multiporosa*
 392 ($\varphi = 0.0518$, 95% CI = 0.030–0.074; Figure 2; Table 1). This estimate of ~5.2% nuDNA
 393 introgression is low and in the opposite direction to what we expected given evidence of repeated
 394 mtDNA introgression from *multiporosa* to *nanamulti*. The unidirectional model from *multiporosa*
 395 to *nanamulti* received only modest support ($B_{10} = 12.26$) with lower introgression estimates ($\varphi =$
 396 0.031, 95% CI = 0.017–0.046). All other introgression scenarios were poorly supported ($B_{10} < 1$).

397 In contrast to the MSCi results, estimates of excess allele sharing using the ABBA-BABA
 398 approach via *Dsuite* found no support for introgression between *nanamulti* and *multiporosa*
 399 (Figure 3). Excess allele sharing was inferred between the *nana1* branch and each of the three
 400 *occidentalis* lineages, with estimates of up to 7% excess allele sharing. However, following
 401 recommendations by Malinsky et al. (2021) to implement FDR P-value adjustment and using $P <$
 402 0.01 as the threshold for statistical significance, no excess allele sharing scenarios were
 403 supported as statistically significant ($P = 0.017$ –0.804; Table S6).

404

405 **Table 1.** Results of MSCi phylogenetic network analysis using BPP. The ‘Model’ column shows
 406 whether the respective analysis tested unidirectional introgression (UDI) or bidirectional
 407 introgression (BDI). Values are the posterior means and 95% credible intervals (in parentheses)
 408 for introgression probability (φ) and introgression time (τ), followed by Bayes factor (B_{10}) support.

Model	Donor	Recipient	φ	$\tau(10^{-3})$	B_{10}
UDI	<i>multiporosa</i>	<i>nanamulti</i>	0.0315 (0.0173–0.0461)	1.255 (1.032–1.468)	12.26
UDI	<i>nanamulti</i>	<i>multiporosa</i>	0.0518 (0.0304–0.0746)	1.287 (1.092–1.499)	∞
BDI	<i>multiporosa</i>	<i>nanamulti</i>	0.0219 (0.0098–0.0349)	1.387 (1.157–1.606)	0.90
BDI	<i>nanamulti</i>	<i>multiporosa</i>	0.0397 (0.0171–0.0636)	1.387 (1.157–1.606)	0.06
UDI	<i>multiporosa</i>	<i>occidentalis-OR</i>	0.0099 (0.0015–0.0189)	0.861 (0.746–0.971)	0.00
UDI	<i>occidentalis-OR</i>	<i>multiporosa</i>	0.0198 (0.0069–0.0334)	0.896 (0.786–0.996)	0.01
BDI	<i>multiporosa</i>	<i>occidentalis-OR</i>	0.0089 (0.0009–0.018)	0.915 (0.814–1.01)	0.01
BDI	<i>occidentalis-OR</i>	<i>multiporosa</i>	0.0204 (0.006–0.035)	0.915 (0.814–1.01)	0.00
UDI	<i>occidentalis-YI</i>	<i>occidentalis-KL</i>	0.0197 (0.0043–0.0201)	0.8 (0.668–0.922)	0.00
UDI	<i>occidentalis-KL</i>	<i>occidentalis-YI</i>	0.02 (0.00816–0.0321)	0.652 (0.533–0.774)	0.02
BDI	<i>occidentalis-YI</i>	<i>occidentalis-KL</i>	0.0095 (0.003–0.0165)	0.742 (0.607–0.864)	0.02
BDI	<i>occidentalis-KL</i>	<i>occidentalis-YI</i>	0.0204 (0.0079–0.0339)	0.742 (0.607–0.864)	0.00



410

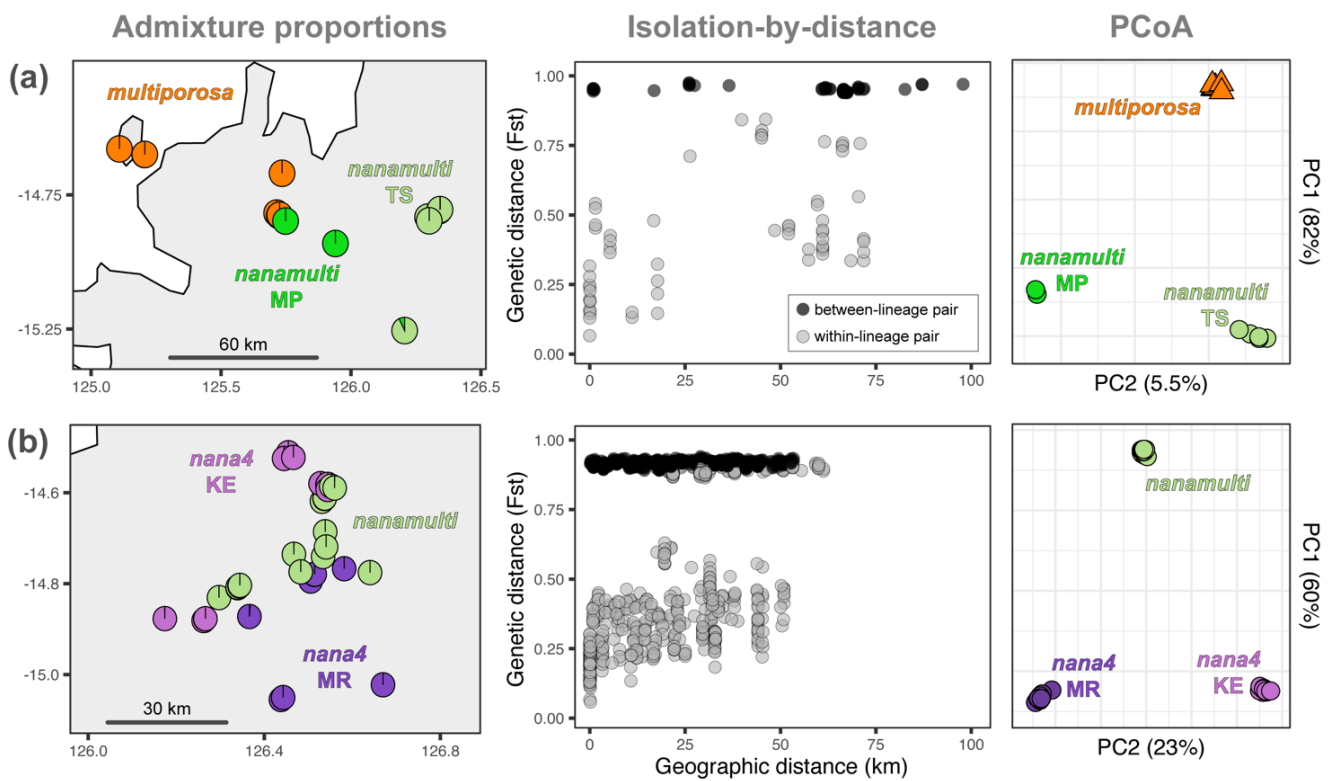
411 **Figure 3.** Excess allele sharing in the *Gehyra nana-occidentalis* clade estimated using f-branch
 412 statistics implemented in *Dsuite*. Colours indicate the proportion of introgressed loci inferred
 413 between the lineage (x axis) and lineage branch (y axis). The f-branch metric accounts for
 414 correlated allele frequencies derived from ancestral introgression using internal branches on the
 415 y-axis (dotted lines). Grey cells represent duplicate or untestable relationships. Note that despite
 416 the ca. 5–7% estimated excess allele sharing between *nana1* and the three *G. occidentalis*
 417 lineages, these were not significant following P-value adjustment (Table S6).

418

419 Recent introgression at contact zones

420 We detected only a single early generation hybrid using NewHybrids, which was between
 421 nanamulti and *nana4* (F1 or F2 hybrid; Table S2; Figure S1), although the sample itself did not
 422 originate from our densely sampled contact for that lineage pair (as shown in Figure 4b). Using
 423 sNMF, optimum K values (based on lowest ce score; Figure S6) were K = 3 for the
 424 nanamulti/*nana4* contact zone, and K = 2 for the *multiporosa*/nanamulti contact zone. In the
 425 case of the *multiporosa*/nanamulti contact zone, however, K = 2 is likely favoured over K = 3 only

426 because of the small sample size ($n = 2$) for what we refer to as the Mitchell Plateau (MP)
 427 population of *nanamulti* (Figure 4a, S7). IBD plots show elevated pairwise F_{ST} between *nanamulti*
 428 samples from MP and the Theda Station (TS) population, with no indication that this is driven by
 429 introgression from *multiporosa*, which would be expected to result in relatively lower F_{ST} between
 430 some between-lineage pairs. Furthermore, the MP and TS samples form distinct clusters in the
 431 PCoA plot (Figure 4a). Considering these points, we opted to use $K = 3$ for this contact zone,
 432 under which sNMF inferred no admixed individuals. Similarly, there is no evidence of admixture at
 433 the *nana4*/*nanamulti* contact zone (Figure 4b), with IBD plots again showing no decrease in
 434 between-lineage pairwise F_{ST} as geographic distance decreases. At this contact zone there is
 435 strong geographic structure within *nana4*, with one population restricted to the King Edward (KE)
 436 sandstones and another restricted to the Morgan River (MR) sandstones.
 437

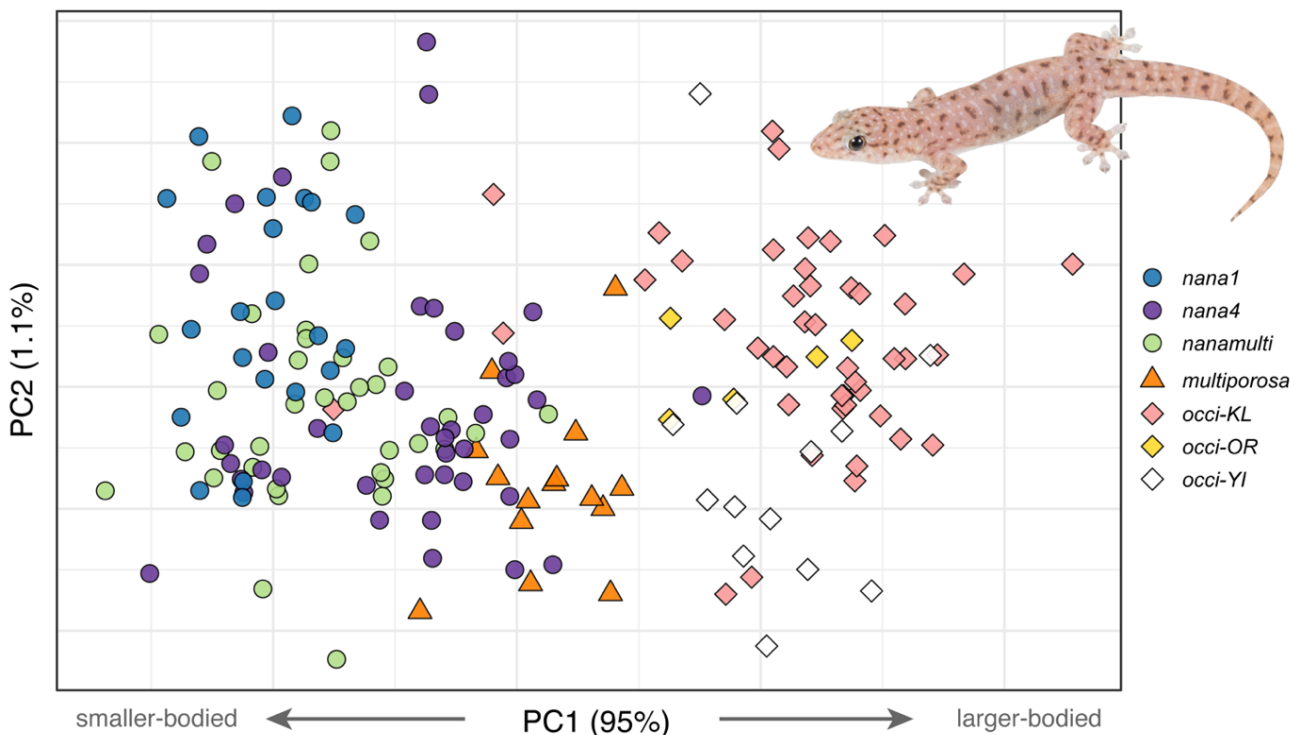


438
 439 **Figure 4.** Estimates of gene flow at contact zones between (a) *multiporosa* and *nanamulti*, and (b)
 440 *nana4* and *nanamulti*. Maps (left column) show pie charts that reflect individual admixture
 441 proportions estimated by sNMF (some charts are slightly offset for visibility). Isolation-by-
 442 distance plots (middle column) illustrate within-lineage (grey) and between-lineage (black).
 443 Principal coordinates analysis plots (right column) illustrate the major axes of genomic variation
 444 for the respective samples. Note that one lineage at each contact zone is represented by two
 445 within-lineage populations, reflecting strong within-lineage geographic structure.
 446

447 Phenotypic variation

448 There was significant morphological divergence among lineages (RRPP: $df = 6/173$ $F = 107.7$, $Z =$
449 17.19 , $R^2 = 0.789$, $P < 0.001$), with lineage accounting for 79% of observed morphological
450 variation. Subsequent pairwise comparisons between lineages found all lineage comparisons –
451 with the exceptions of *multiporosa* + *occidentalis*-OR, *nana1* + *nanamulti*, *nana4* + *nanamulti*,
452 and all *occidentalis* lineage comparisons – to be significantly different ($P < 0.05$; Table S7).
453 Principal components (PC) axes indicate that body size is the main axis of morphological
454 variation among lineages (Figure 5), with all traits loading heavily on PC1 (Table S8), which
455 accounts for 95% of morphological variation. Body shape overlapped considerably among
456 lineages (Figure 5). PC2 explained only 1.1% of variation, with head depth loading most heavily.
457 PC3 explained 0.96% of variation, with (in descending order) width-between-eyes, forelimb
458 length, and hindlimb length loading most heavily. A total of 98% of morphological variation was
459 explained by PC1–3 (Table S8). Finally, while body size varied among lineages, there were no
460 significant differences in body size variance among lineages (Fligner-Killeen test: $X^2 = 11.749$, $df =$
461 6 , $P = 0.068$).

462



463

464 **Figure 5.** Principal Components Analysis of morphological variation across focal lineages in the
465 *Gehyra nana-occidentalis* clade. Individuals are coloured according to their nuDNA ancestry.
466 Percent variation explained for each axis. An individual of *nana1* is shown (credit: Scott Macor).

467

468

469 Discussion

470 In this study we found extensive, within-lineage mitonuclear discordance consistent with
471 repeated mitochondrial introgression from *G. multiporosa* to *nanamulti*. We also confirmed
472 phylogenetic-scale mitonuclear discordance in the *G. occidentalis* complex that could reflect
473 either of two equivocal scenarios of mtDNA introgression; although here mtDNA introgression,
474 rather than ILS, is less certain than between *multiporosa* and *nanamulti*. Despite these cases of
475 mitonuclear discordance, phylogenetic network analysis strongly supported only a single
476 instance of modest nuDNA introgression — from *nanamulti* to *multiporosa*, in the opposite
477 direction to mitochondrial capture — but with no congruent support from *D*-statistics.
478 Furthermore, we found no evidence of recent or ongoing introgression between lineages at the
479 two contact zones examined here (Figure 5), including between *multiporosa* and *nanamulti*
480 where they currently co-occur; although we did detect a single early generation hybrid between
481 *nana4* and *nanamulti*. Finally, we found evidence of novel, intermediate, or more variable
482 morphological traits in lineages with mitonuclear discordance. Collectively, these results
483 highlight a system with clear evidence of repeated hybridisation and mtDNA capture but with no
484 overt evidence of other genotypic or phenotypic consequences. We note that our use of protein-
485 coding exon data could have missed introgressed regions of the genome; however, we might still
486 have expected our *Dsuite* analysis, which used genome-wide SNP data, to identify potential
487 nuDNA introgression. Further studies in this system could use complete genome sequencing to
488 compare nuDNA regions associated with mitonuclear interactions, as co-introgression of these
489 alleles may be necessary to maintain mitochondrial performance (Ding et al., 2021; Nikelski et
490 al., 2023).

491

492 Mitonuclear discordance but no substantial nuclear introgression

493 Mitonuclear discordance is often an indicator of mtDNA introgression (Toews & Brelsford, 2012)
494 and frequently predicts matching nuDNA introgression (e.g., Sarver et al., 2021; Ji et al., 2023;
495 Potter et al., 2024). However, widespread mtDNA introgression can also occur with
496 comparatively low levels of nuDNA introgression (Chan & Levin, 2005; Sloan et al., 2017). Here,
497 our results add to a growing body of evidence demonstrating mtDNA introgression with little
498 concomitant nuDNA introgression, which has been identified widely across taxa (e.g., Nevado et
499 al., 2009; Boratyński et al., 2015; Good et al., 2015; Grummer et al., 2018; Mao & Rossiter, 2020).
500 However, complete, recurrent mtDNA replacement with no detected nuDNA introgression – as
501 observed here for *nanamulti* – seems markedly rarer and, to the best of our knowledge, has only
502 been reported in *Lissotriton* newts (Zieliński et al., 2013).

503 Mitochondrial genomes can easily cross species boundaries following hybridisation due
504 to a lack of recombination and uniparental inheritance (Vargas et al., 2017; Zhang et al., 2019).
505 Within the *nana-occidentalis* clade, mitonuclear discordance observed within nanamulti itself
506 implies multiple, recent introgression events from *multiporosa*. Despite this, we detected only
507 small amounts of nuDNA introgression (~5%) and in the opposite direction — from nanamulti to
508 *multiporosa* — to what was expected given the direction of mtDNA introgression. The
509 discordance within the *occidentalis* complex is more difficult to interpret and could be explained
510 by mtDNA capture from *multiporosa* to *occidentalis*-OR or from *occidentalis*-YI to *occidentalis*-
511 KL — or even by estimation error or incomplete lineage sorting. In this case, we found no
512 evidence of nuDNA introgression to match either scenario of mtDNA introgression. Despite a
513 general lack of nuDNA introgression shown here, repeated instances of mtDNA capture indicate
514 that hybridisation is, or has been, relatively frequent in the *nana-occidentalis* clade. Phylogenies
515 inferred from mtDNA are expected to achieve reciprocal monophyly more quickly than nuDNA
516 due to their elevated mutation rates (Ballard & Whitlock, 2004). This suggests that the mtDNA
517 introgression events from *multiporosa* to nanamulti have been recent given the rampant mtDNA
518 paraphyly within these lineages. Thus, nuDNA introgression was either swiftly purged or
519 extremely limited following these introgression events.

520 Several factors may explain the lack of nuDNA introgression observed here. Adaptive
521 introgression of mtDNA is frequently cited to drive asymmetrical patterns of mtDNA vs nuDNA
522 introgression (Toews & Brelsford, 2012; Bonnet et al., 2017; Sloan et al., 2017) and has been
523 identified in *Lepus* hares (Melo-Ferreira et al., 2014), *Drosophila* flies (Llopart et al., 2014), and
524 *Myodes voles* (Boratyński et al., 2015), among other taxa. However, confident identification of
525 adaptive introgression requires the demonstration of adaptive function, which is often difficult
526 (Taylor & Larson, 2019). Detection methods for positive selection (e.g., Suarez-Gonzalez et al.,
527 2018) must be used with caution, as phenomena such as heterosis can mimic signals of adaptive
528 introgression (Kim et al., 2017). Alternatively, demographic processes such as gene surfing —
529 whereby markers, such as mtDNA, are fixed in populations undergoing rapid range expansion
530 (Excoffier et al., 2009) — may have driven the fixation of *multiporosa* mtDNA in nanamulti, as
531 there is evidence of range expansion in nanamulti (Lau et al., 2024). Similar introgression
532 scenarios driven by range expansion have been detected in groups such as *Otospermophilus*
533 ground squirrels (Phuong et al., 2017) and *Ursus* bears (Cahill et al., 2013). However, range
534 expansion would not account for the fixation of *multiporosa* mtDNA over the entirety of the range
535 of nanamulti, and demographic processes generally have been suggested to cause massive
536 discordance only rarely (see Bonnet et al., 2017).

537

538 Introgression and morphology

539 Despite a growing number of studies demonstrating the potential role introgression can play in
540 generating morphological variation (e.g., Lamichhaney et al., 2015; Taylor & Larson, 2019), we
541 found no association between introgression and phenotypic variation in the *nana-occidentalis*
542 clade in terms of the morphometric characters we measured. However, given the lack of nuDNA
543 introgression found here, it is not surprising that we found no evidence for transgressive,
544 intermediate, or more variable phenotypes. In other cases where introgression has been
545 suggested to influence morphology in squamates (e.g., Pavón-Vázquez et al., 2021; Wogan et al.,
546 2023) the estimated proportion of introgression was significantly higher than what was found
547 here. In line with other studies of *Gehyra* morphology (see Siström et al., 2012; Kealley et al.,
548 2018; Moritz et al., 2018), our results highlighted body size as the main axis of among-lineage
549 morphological variation in the *nana-occidentalis* clade. Considering this, it is worth noting that
550 *multiporosa* is somewhat intermediate in body size with respect to the *nana* and *occidentalis*
551 complexes. This could have facilitated hybridisation with *nanamulti* or it could, conceivably, be
552 the result of introgression; however, this is unlikely considering the modest nuDNA introgression
553 estimated using the MSCi, and the lack of introgression detected with *D*-statistics.

554

555 Conclusions and future directions

556 Methods to infer genomic introgression have improved and diversified over the last two decades
557 and, given the biases and limitations unique to each method, comparing the results of multiple
558 analyses is often warranted to ensure that results are robust (Hibbins & Hahn, 2022). Here, we
559 used several such methods to understand the complicated evolutionary history of a clade of
560 *Gehyra* geckos. These results highlight a system with repeated instances of asymmetrical mtDNA
561 introgression with limited evidence of corresponding nuDNA introgression. Mitonuclear
562 discordance and introgression have now been widely identified in squamates (e.g., Grummer et
563 al., 2018; Prates et al., 2023; Wogan et al., 2023; Myers et al., 2024), however, in none of these
564 instances has the disparity between levels of mtDNA and nuDNA introgression been so clearly
565 demonstrated. More work in this and other systems is needed to understand whether such
566 mismatches result from selection or non-adaptive factors. such studies could also assess the
567 potential for mtDNA introgression to drive speciation by providing adaptive benefit, or by
568 introducing mitonuclear interactions that reinforce RI between diverging lineages. Whole genome
569 sequencing is more accessible than ever and will be needed to answer such questions
570 (Combrink et al., 2025).

571

572 **Acknowledgments**

573 We thank Scott Macor and Naomi Laven for assistance with field sampling; Adam Leaché, Emily
574 Roycroft, Kate O’Hara, and Rhiannon Schembri for advice; Rhiannon Schembri for assistance
575 with lab work; Paul Doughty and Kailah Thorn of the Western Australian Museum for access to
576 tissues and specimens; and Scott Macor and Ian Bool for providing photos. This work was funded
577 by Australian Research Council Discovery Projects DP190102395 and DP210102267, and an
578 Australian Biological Resources Study NTRGP Postdoctoral Fellowship Grant to SMZ
579 (NTRGI000036).

580

581 **References**

- 582 Abbott, R., Albach, D., Ansell, S., Arntzen, J. W., Baird, S. J., Bierne, N., Boughman, J., Brelsford, A.,
583 Buerkle, C. A., Buggs, R., Butlin, R. K., Dieckmann, U., Eroukhmanoff, F., Grill, A., Cahan, S. H.,
584 Hermansen, J. S., Hewitt, G., Hudson, A. G., Jiggins, C., Jones, J., Keller, B., Marczewski, T., Mallet, J.,
585 Martinez-Rodriguez, P., Möst, M., Mullen, S., Nichols, R., Nolte, A. W., Parisod, C., Pfennig, K., Rice, A.
586 M., Ritchie, M. G., Seifert, B., Smadja, C. M., Stelkens, R., Szymura, J. M., Väinölä, R., Wolf, J. B., &
587 Zinner, D. (2013). Hybridization and speciation. *Journal of Evolutionary Biology*, 26(2), 229–246.
588 <https://doi.org/10.1111/j.1420-9101.2012.02599.x>
- 589 Anderson, E., & Thompson, E. (2002). A model-based method for identifying species hybrids using
590 multilocus genetic data. *Genetics*, 160(3), 1217–1229.
- 591 Ashman, L., Bragg, J., Doughty, P., Hutchinson, M., Bank, S., Matzke, N., Oliver, P., & Moritz, C. (2018).
592 Diversification across biomes in a continental lizard radiation. *Evolution*, 72(8), 1553–1569.
- 593 Ballard, J. W., & Whitlock, M. C. (2004). The incomplete natural history of mitochondria. *Molecular*
594 *Ecology*, 13(4), 729–744. <https://doi.org/10.1046/j.1365-294x.2003.02063.x>
- 595 Barley, A. J., Nieto-Montes de Oca, A., Manríquez-Morán, N. L., & Thomson, R. C. (2024). Understanding
596 Species Boundaries that Arise from Complex Histories: Gene Flow Across the Speciation Continuum in
597 the Spotted Whiptail Lizards. *Systematic Biology*, 73(6), 901–919.
- 598 Benjamini, Y., & Hochberg, Y. (1995). Controlling the False Discovery Rate: A Practical and Powerful
599 Approach to Multiple Testing. *Journal of the Royal Statistical Society: Series B (Methodological)*, 57(1),
600 289–300. <https://doi.org/10.1111/j.2517-6161.1995.tb02031.x>
- 601 Blom, M. P. (2015). EAPhy: a flexible tool for high-throughput quality filtering of exon-alignments and data
602 processing for phylogenetic methods. *PLoS Currents*, 5(7).
603 <https://doi.org/10.1371/currents.tol.75134257bd389c04bc1d26d42aa9089f>
- 604 Bonnet, T., Leblois, R., Rousset, F., & Crochet, P. A. (2017). A reassessment of explanations for discordant
605 introgressions of mitochondrial and nuclear genomes. *Evolution*, 71(9), 2140–2158.

606 Boratyński, Z., Melo-Ferreira, J., Alves, P., Berto, S., Koskela, E., Pentikäinen, O., Tarroso, P., Ylilauri, M., &
607 Mappes, T. (2014). Molecular and ecological signs of mitochondrial adaptation: consequences for
608 introgression? *Heredity*, 113(4), 277–286.

609 Bradburd, G. (2013). Package ‘BEDASSLE’. Comprehensive R Archive Network.

610 Cahill, J. A., Green, R. E., Fulton, T. L., Stiller, M., Jay, F., Ovsyanikov, N., Salamzade, R., St. John, J., Stirling,
611 I., & Slatkin, M. (2013). Genomic evidence for island population conversion resolves conflicting
612 theories of polar bear evolution. *PLoS Genetics*, 9(3), e1003345.

613 Chan, K. M. A., & Levin, S. A. (2005). Leaky prezygotic isolation and porous genomes: rapid introgression of
614 maternally inherited DNA. *Evolution*, 59(4), 720–729. [https://doi.org/10.1111/j.0014-](https://doi.org/10.1111/j.0014-3820.2005.tb01748.x)
615 [3820.2005.tb01748.x](https://doi.org/10.1111/j.0014-3820.2005.tb01748.x)

616 Collyer, M. L., Sekora, D. J., & Adams, D. C. (2015). A method for analysis of phenotypic change for
617 phenotypes described by high-dimensional data. *Heredity*, 115(4), 357–365.
618 <https://doi.org/10.1038/hdy.2014.75>

619 Combrink, L. L., Golcher-Benavides, J., Lewanski, A. L., Rick, J. A., Rosenthal, W. C., & Wagner, C. E.
620 (2025). Population Genomics of Adaptive Radiation. *Molecular Ecology*, 34, e17574.

621 Cooper, E. D. (2014). Overly simplistic substitution models obscure green plant phylogeny. *Trends in Plant*
622 *Science*, 19(9), 576–582.

623 Cruickshank, T. E., & Hahn, M. W. (2014). Reanalysis suggests that genomic islands of speciation are due
624 to reduced diversity, not reduced gene flow. *Molecular Ecology*, 23(13), 3133–3157.

625 Currat, M., Ruedi, M., Petit, R. J., & Excoffier, L. (2008). The hidden side of invasions: massive introgression
626 by local genes. *Evolution*, 62(8), 1908–1920. <https://doi.org/10.1111/j.1558-5646.2008.00413.x>

627 Dickey, M. (1971). The weighted likelihood ratio, linear hypotheses on normal location parameters. *The*
628 *Annals of Mathematical Statistics*, 42(1), 204–223.

629 Ding, Y., Chen, W., Li, Q., Rossiter, S. J., & Mao, X. (2021). Mitonuclear mismatch alters nuclear gene
630 expression in naturally introgressed *Rhinolophus bats*. *Frontiers in Zoology*, 18, 1–14.

631 Dittrich-Reed, D. R., & Fitzpatrick, B. M. (2013). Transgressive hybrids as hopeful monsters. *Evolutionary*
632 *Biology*, 40, 310–315.

633 Dixon, P. (2003). VEGAN, a package of R functions for community ecology. *Journal of Vegetation Science*,
634 14, 927–930. [https://doi.org/10.1658/1100-9233\(2003\)014\[0927:VAPORF\]2.0.CO;2](https://doi.org/10.1658/1100-9233(2003)014[0927:VAPORF]2.0.CO;2)

635 Doughty, P., Bourke, G., Tedeschi, L. G., Pratt, R. C., Oliver, P. M., Palmer, R. A., & Moritz, C. (2018). Species
636 delimitation in the *Gehyra nana* (Squamata: Gekkonidae) complex: cryptic and divergent
637 morphological evolution in the Australian Monsoonal Tropics, with the description of four new species.
638 *Zootaxa*, 4403(2), 201–244. <https://doi.org/10.11646/zootaxa.4403.2.1>

639 Doughty, P., Palmer, R., Sistrom, M. J., Bauer, A. M., & Donnellan, S. C. (2012). Two new species of *Gehyra*
640 (Squamata: Gekkonidae) geckos from the north-west Kimberley region of Western Australia. *Records of*
641 *the Western Australian Museum*, 27(2), 117–134.

642 Durand, E. Y., Patterson, N., Reich, D., & Slatkin, M. (2011). Testing for ancient admixture between closely
643 related populations. *Molecular Biology and Evolution*, 28(8), 2239–2252.
644 <https://doi.org/10.1093/molbev/msr048>

645 Edelman, N. B., & Mallet, J. (2021). Prevalence and Adaptive Impact of Introgression. *Annual Review of*
646 *Genetics*, 55, 265–283. <https://doi.org/10.1146/annurev-genet-021821-020805>

647 Excoffier, L., Foll, M., & Petit, R. J. (2009). Genetic consequences of range expansions.
648 *Annual Review of Ecology, Evolution, and Systematics*, 40(1), 481–501.

649 Fenker, J., Tedeschi, L. G., Melville, J., & Moritz, C. (2021). Predictors of phylogeographic structure among
650 codistributed taxa across the complex Australian monsoonal tropics. *Molecular Ecology*, 30(17), 4276–
651 4291. <https://doi.org/10.1111/mec.16057>

652 Fligner, M. A., & Killeen, T. J. (1976). Distribution-Free Two-Sample Tests for Scale. *Journal of the American*
653 *Statistical Association*, 71(353), 210–213. <https://doi.org/10.2307/2285771>

654 Flouri, T., Jiao, X., Rannala, B., & Yang, Z. (2018). Species Tree Inference with BPP Using Genomic
655 Sequences and the Multispecies Coalescent. *Molecular Biology and Evolution*, 35(10), 2585–2593.
656 <https://doi.org/10.1093/molbev/msy147>

657 Flouri, T., Jiao, X., Rannala, B., & Yang, Z. (2020). A Bayesian Implementation of the Multispecies
658 Coalescent Model with Introgression for Phylogenomic Analysis. *Molecular Biology and Evolution*,
659 37(4), 1211–1223. <https://doi.org/10.1093/molbev/msz296>

660 Frichot, E., Mathieu, F., Trouillon, T., Bouchard, G., François, O. (2014). Fast and Efficient Estimation of
661 Individual Ancestry Coefficients. *Genetics*, 196(4), 973–983.
662 <https://doi.org/10.1534/genetics.113.160572>

663 Frichot, E., & François, O. (2015). LEA: An R Package for Landscape and Ecological Association Studies.
664 *Methods in Ecology and Evolution*, 6(8), 925–929. <https://doi.org/10.1111/2041-210X.12382>

665 Gadagkar, S. R., Rosenberg, M. S., & Kumar, S. (2005). Inferring species phylogenies from multiple genes:
666 concatenated sequence tree versus consensus gene tree. *Journal of Experimental Zoology Part B:*
667 *Molecular and Developmental Evolution*, 304(1), 64–74.

668 Galtier, N., & Daubin, V. (2008). Dealing with incongruence in phylogenomic analyses. *Philosophical*
669 *Transactions of the Royal Society B: Biological Sciences*, 363(1512), 4023–4029.

670 Good, J. M., Vanderpool, D., Keeble, S., & Bi, K. (2015). Negligible nuclear introgression despite complete
671 mitochondrial capture between two species of chipmunks. *Evolution*, 69(8), 1961–1972.

672 Gruber, B., Unmack, P. J., Berry, O. F., & Georges, A. (2018). dartr: An r package to facilitate analysis of SNP
673 data generated from reduced representation genome sequencing. *Molecular Ecology Resources*, 18(3),
674 691–699.

675 Grummer, J. A., Morando, M. M., Avila, L. J., Sites, J. W., & Leaché, A. D. (2018). Phylogenomic evidence for
676 a recent and rapid radiation of lizards in the Patagonian *Liolaemus fitzingerii* species group. *Molecular*
677 *Phylogenetics and Evolution*, 125, 243–254.
678 <https://doi.org/https://doi.org/10.1016/j.ympev.2018.03.023>

679 Guindon, S., Dufayard, J.-F., Lefort, V., Anisimova, M., Hordijk, W., & Gascuel, O. (2010). New algorithms
680 and methods to estimate maximum-likelihood phylogenies: assessing the performance of PhyML 3.0.
681 *Systematic Biology*, 59(3), 307–321.

682 Harrison, R. G., & Larson, E. L. (2014). Hybridization, introgression, and the nature of species boundaries.
683 *Journal of Heredity*, 105(S1), 795–809.

684 Heinicke, M., Greenbaum, E., Jackman, T., & Bauer, A. (2011). Phylogeny of a trans-Wallacean radiation
685 (Squamata, Gekkonidae, *Gehyra*) supports a single early colonization of Australia. *Zoologica Scripta*,
686 40, 584–602. <https://doi.org/10.1111/j.1463-6409.2011.00495.x>

687 Hibbins, M. S., & Hahn, M. W. (2022). Phylogenomic approaches to detecting and characterizing
688 introgression. *Genetics*, 220(2), iyab173. <https://doi.org/10.1093/genetics/iyab173>

689 Hill, G. E. (2019). Reconciling the mitonuclear compatibility species concept with rampant mitochondrial
690 introgression. *Integrative and Comparative Biology*, 59(4), 912–924.

691 Hillis, D. M., Chambers, E. A., & Devitt, T. J. (2021). Contemporary methods and evidence for species
692 delimitation. *Ichthyology & Herpetology*, 109(3), 895–903.

693 Hoang, D. T., Chernomor, O., Von Haeseler, A., Minh, B. Q., & Vinh, L. S. (2018). UFBoot2: improving the
694 ultrafast bootstrap approximation. *Molecular Biology and Evolution*, 35(2), 518–522.

695 Hodcroft, E. (2016). TreeCollapserCL4. Retrieved 10/05/2023 from
696 <http://emmahodcroft.com/TreeCollapseCL.html>

697 Huang, J., Thawornwattana, Y., Flouri, T., Mallet, J., & Yang, Z. (2022). Inference of Gene Flow between
698 Species under Misspecified Models. *Molecular Biology and Evolution*, 39(12), msac237.
699 <https://doi.org/10.1093/molbev/msac237>

700 Ji, J., Jackson, D. J., Leaché, A. D., & Yang, Z. (2023). Power of Bayesian and Heuristic Tests to Detect
701 Cross-Species Introgression with Reference to Gene Flow in the *Tamias quadrivittatus* Group of North
702 American Chipmunks. *Systematic Biology*, 72(2), 446–465. <https://doi.org/10.1093/sysbio/syac077>

703 Kalyaanamoorthy, S., Minh, B. Q., Wong, T. K. F., von Haeseler, A., & Jermini, L. S. (2017). ModelFinder: fast
704 model selection for accurate phylogenetic estimates. *Nature Methods*, 14(6), 587–589.
705 <https://doi.org/10.1038/nmeth.4285>

706 Kealley, L., Doughty, P., Pepper, M., Keogh, J. S., Hillyer, M., & Huey, J. (2018). Conspicuously concealed:
707 revision of the arid clade of the *Gehyra variegata* (Gekkonidae) group in Western Australia using an
708 integrative molecular and morphological approach, with the description of five cryptic species. *PeerJ*,
709 6, e5334. <https://doi.org/10.7717/peerj.5334>

710 Kilian, A., Wenzl, P., Huttner, E., Carling, J., Xia, L., Blois, H., Caig, V., Heller-Uszynska, K., Jaccoud, D.,
711 Hopper, C., Aschenbrenner-Kilian, M., Evers, M., Peng, K., Cayla, C., Hok, P., Uszynski, G. (2012).
712 Diversity arrays technology: a generic genome profiling technology on open platforms. *Data production
713 and analysis in population genomics: Methods and protocols*, 67–89.

714 Kim, B. Y., Huber, C. D., & Lohmueller, K. E. (2017). Deleterious variation mimics signatures of genomic
715 incompatibility and adaptive introgression. *PLOS Genetics*, 14(10),
716 e1007741. <https://doi.org/10.1371/journal.pgen.1007741>

717 Lamichhaney, S., Berglund, J., Almén, M. S., Maqbool, K., Grabherr, M., Martinez-Barrio, A., Promerová, M.,
718 Rubin, C. J., Wang, C., Zamani, N., Grant, B. R., Grant, P. R., Webster, M. T., & Andersson, L. (2015).
719 Evolution of Darwin's finches and their beaks revealed by genome sequencing. *Nature*, 518(7539), 371–
720 375. <https://doi.org/10.1038/nature14181>

721 Lanfear, R., Calcott, B., Ho, S. Y., & Guindon, S. (2012). PartitionFinder: combined selection of partitioning
722 schemes and substitution models for phylogenetic analyses. *Molecular Biology and Evolution*, 29(6),
723 1695–1701.

724 Larson, D. A., Itgen, M., Denton, R., & Hahn, M. W. (preprint). Reconsidering cytonuclear discordance in
725 the genomic age. *EcoEvoRxiv*. <https://doi.org/https://doi.org/10.32942/X2KG8R>

726 Lau, C. C., Christian, K. A., Fenker, J., Laver, R. J., O'Hara, K., Zozaya, S. M., Moritz, C., & Roycroft, E.
727 (2024). Range size variably predicts genetic diversity in *Gehyra* geckos. *EcoEvoRxiv*.
728 <https://doi.org/10.32942/X2PW49>

729 Lawson, D. J., van Dorp, L., & Falush, D. (2018). A tutorial on how not to over-interpret STRUCTURE and
730 ADMIXTURE bar plots. *Nature Communications*, 9(1), 3258. [https://doi.org/10.1038/s41467-018-](https://doi.org/10.1038/s41467-018-05257-7)
731 [05257-7](https://doi.org/10.1038/s41467-018-05257-7)

732 Llopart, A., Herrig, D., Brud, E., & Stecklein, Z. (2014). Sequential adaptive introgression of the
733 mitochondrial genome in *Drosophila yakuba* and *Drosophila santomea*. *Molecular Ecology*, 23(5),
734 1124–1136.

735 Malinsky, M., Matschiner, M., & Svardal, H. (2021). Dsuite - Fast D-statistics and related admixture
736 evidence from VCF files. *Molecular Ecology Resources*, 21(2), 584–595. [https://doi.org/10.1111/1755-](https://doi.org/10.1111/1755-0998.13265)
737 [0998.13265](https://doi.org/10.1111/1755-0998.13265)

738 Mallet, J., Besansky, N., & Hahn, M. W. (2016). How reticulated are species? *BioEssays*, 38(2), 140–149.

739 Mao, X., & Rossiter, S. J. (2020). Genome-wide data reveal discordant mitonuclear introgression in the
740 intermediate horseshoe bat (*Rhinolophus affinis*). *Molecular Phylogenetics and Evolution*, 150,
741 106886.

742 Masello, J. F., Quillfeldt, P., Sandoval-Castellanos, E., Alderman, R., Calderón, L., Cherel, Y., Cole, T. L.,
743 Cuthbert, R. J., Marin, M., & Massaro, M. (2019). Additive traits lead to feeding advantage and
744 reproductive isolation, promoting homoploid hybrid speciation. *Molecular Biology and Evolution*, 36(8),
745 1671–1685.

746 Mayr, E. (1963). Animal species and evolution. *Harvard University Press*.

747 Melo-Ferreira, J., Vilela, J., Fonseca, M. M., da Fonseca, R. R., Boursot, P., & Alves, P. C. (2014). The elusive
748 nature of adaptive mitochondrial DNA evolution of an arctic lineage prone to frequent introgression.
749 *Genome Biology and Evolution*, 6(4), 886–896.

750 Minh, B. Q., Schmidt, H. A., Chernomor, O., Schrempf, D., Woodhams, M. D., Von Haeseler, A., & Lanfear,
751 R. (2020). IQ-TREE 2: new models and efficient methods for phylogenetic inference in the genomic era.
752 *Molecular Biology and Evolution*, 37(5), 1530–1534.

753 Moritz, C. C., Pratt, R. C., Bank, S., Bourke, G., Bragg, J. G., Doughty, P., Keogh, J. S., Laver, R. J., Potter, S.,
754 Teasdale, L. C., Tedeschi, L. G., & Oliver, P. M. (2018). Cryptic lineage diversity, body size divergence,
755 and sympatry in a species complex of Australian lizards (*Gehyra*). *Evolution*, 72(1), 54–66.
756 <https://doi.org/10.1111/evo.13380>

757 Myers, E., Rautsaw, R., Borja, M., Jones, J., Grunwald, C., Holding, M., Graziotin, F., & Parkinson, C.
758 (2024). Phylogenomic discordance is driven by widespread introgression and incomplete lineage
759 sorting during rapid species diversification within Rattlesnakes (Viperidae: *Crotalus* and *Sistrurus*).
760 *Systematic Biology*, 73(4), 722–741.

761 Nevado, B., Koblmüller, S., Sturmbauer, C., Snoeks, J., Usano-Aleman, J., & Verheyen, E. (2009).
762 Complete mitochondrial DNA replacement in a Lake Tanganyika cichlid fish. *Molecular Ecology*, 18(20),
763 4240–4255.

764 Nikelski, E., Rubtsov, A. S., & Irwin, D. (2023). High heterogeneity in genomic differentiation between
765 phenotypically divergent songbirds: a test of mitonuclear co-introgression. *Heredity*, 130(1), 1–13.

766 Oliver, P., Laver, R., Martins, F., Pratt, R., Hunjan, S., & Moritz, C. (2016). A novel hotspot of vertebrate
767 endemism and an evolutionary refugium in tropical Australia. *Diversity and Distributions*, 23(1), 53–66.
768 <https://doi.org/10.1111/ddi.12506>

769 Oliver, P. M., Prasetya, A. M., Tedeschu, L. G., Fenker, J., Ellis, R. J., Doughty, P., & Moritz, C. (2020). Cryptic
770 and convergence: integrative taxonomic revision of the *Gehyra australis* group (Squamata: Gekkonidae)
771 from northern Australia. *PeerJ*, 8, e7971. <https://doi.org/10.7717/peerj.7971>

772 Patterson, N., Moorjani, P., Luo, Y., Mallick, S., Rohland, N., Zhan, Y., Genschoreck, T., Webster, T., &
773 Reich, D. (2012). Ancient admixture in human history. *Genetics*, 192(3), 1065–1093.

774 Pavón-Vázquez, C. J., Rana, Q., Farleigh, K., Crispo, E., Zeng, M., Lilliah, J., Mulcahy, D., Ascanio, A.,
775 Jezkova, T., & Leaché, A. D. (2024). Gene Flow and Isolation in the Arid Nearctic Revealed by Genomic
776 Analyses of Desert Spiny Lizards. *Systematic Biology*, 73(2), 323–342.
777 <https://doi.org/10.1093/sysbio/syae001>

778 Phuong, M. A., Bi, K., & Moritz, C. (2017). Range instability leads to cytonuclear discordance in a
779 morphologically cryptic ground squirrel species complex. *Molecular Ecology*, 26(18), 4743–4755.

780 Potter, S., Moritz, C., Piggott, M. P., Bragg, J. G., Afonso Silva, A. C., Bi, K., McDonald-Spicer, C., Turakulov,
781 R., & Eldridge, M. D. (2024). Museum skins enable identification of introgression associated with
782 cytonuclear discordance. *Systematic Biology*, 73(3), 579–593. <https://doi.org/10.1093/sysbio/syae016>

783 Prates, I., Hutchinson, M. N., Singhal, S., Moritz, C., & Rabosky, D. L. (2023). Notes from the taxonomic
784 disaster zone: Evolutionary drivers of intractable species boundaries in an Australian lizard clade
785 (Scincidae: *Ctenotus*). *Molecular Ecology*, 33(20), e17074. <https://doi.org/10.1111/mec.17074>

786 Puechmaille, S. J. (2016). The program structure does not reliably recover the correct population structure
787 when sampling is uneven: subsampling and new estimators alleviate the problem. *Molecular Ecology*
788 *Resources*, 16(3), 608–627. <https://doi.org/10.1111/1755-0998.12512>

789 Rabiee, M., Sayyari, E., & Mirarab, S. (2019). Multi-allele species reconstruction using ASTRAL. *Molecular*
790 *Phylogenetics and Evolution*, 130, 286–296.
791 <https://doi.org/https://doi.org/10.1016/j.ympev.2018.10.033>

792 Rambaut, A., Drummond, A. J., Xie, D., Baele, G., & Suchard, M. A. (2018). Posterior summarization in
793 Bayesian phylogenetics using Tracer 1.7. *Systematic Biology*, 67(5), 901–904.

794 Rhymer, J. M., & Simberloff, D. (1996). Extinction by Hybridization and Introgression. *Annual Review of*
795 *Ecology and Systematics*, 27, 83–109. <http://www.jstor.org/stable/2097230>

796 Sansaloni, C. P., Petrolì, C. D., Carling, J., Hudson, C. J., Steane, D. A., Myburg, A. A., Grattapaglia, D.,
797 Vaillancourt, R. E., & Kilian, A. (2010). A high-density Diversity Arrays Technology (DArT) microarray for
798 genome-wide genotyping in Eucalyptus. *Plant Methods*, 6, 1–11.

799 Sarver, B. A. J., Herrera, N. D., Sneddon, D., Hunter, S. S., Settles, M. L., Kronenberg, Z., Demboski, J. R.,
800 Good, J. M., & Sullivan, J. (2021). Diversification, Introgression, and Rampant Cytonuclear Discordance
801 in Rocky Mountains Chipmunks (Sciuridae: *Tamias*). *Systematic Biology*, 70(5), 908–921.
802 <https://doi.org/10.1093/sysbio/syaa085>

803 Schumer, M., Rosenthal, G. G., & Andolfatto, P. (2014). How common is homoploid hybrid speciation?
804 *Evolution*, 68(6), 1553–1560. <https://doi.org/10.1111/evo.12399>

805 Seo, T.-K., Kishino, H., & Thorne, J. L. (2005). Incorporating gene-specific variation when inferring and
806 evaluating optimal evolutionary tree topologies from multilocus sequence data.
807 *Proceedings of the National Academy of Sciences*, 102(12), 4436–4441.

808 Simmons, M. P., & Gatesy, J. (2021). Collapsing dubiously resolved gene-tree branches in phylogenomic
809 coalescent analyses. *Molecular Phylogenetics and Evolution*, 158, 107092.
810 <https://doi.org/https://doi.org/10.1016/j.ympev.2021.107092>

811 Sistrom, M., Edwards, D. L., Donnellan, S., & Hutchinson, M. (2012). Morphological differentiation
812 correlates with ecological but not with genetic divergence in a *Gehyra* gecko. *Journal of Evolutionary*
813 *Biology*, 25(4), 647–660. <https://doi.org/10.1111/j.1420-9101.2012.02460.x>

814 Sistrom, M., Hutchinson, M., Hutchinson, R., & Donnellan, S. (2009). Molecular Phylogeny Of Australian
815 *Gehyra* (Squamata: Gekkonidae) And Taxonomic Revision Of *Gehyra variegata* In South-Eastern
816 Australia. *Zootaxa*, 2277, 14–32. <https://doi.org/10.5281/zenodo.191131>

817 Sloan, D. B., Havird, J. C., & Sharbrough, J. (2017). The on-again, off-again relationship between
818 mitochondrial genomes and species boundaries. *Molecular Ecology*, 26(8), 2212–2236.

819 Smith, M. L., & Hahn, M. W. (2024). Selection leads to false inferences of introgression using popular
820 methods. *Genetics*, 227(4), iyae089.

821 Srivathsan, A., Lee, L., Katoh, K., Hartop, E., Kutty, S. N., Wong, J., Yeo, D., & Meier, R. (2021). ONTbarcoder
822 and MinION barcodes aid biodiversity discovery and identification by everyone, for everyone. *BMC*
823 *biology*, 19, 1–21.

824 Staubach, F., Lorenc, A., Messer, P. W., Tang, K., Petrov, D. A., & Tautz, D. (2012). Genome patterns of
825 selection and introgression of haplotypes in natural populations of the house mouse (*Mus musculus*).
826 *PLoS Genetics*, 8(8), e1002891. <https://doi.org/10.1371/journal.pgen.1002891>

827 Suarez-Gonzalez, A., Lexer, C., & Cronk, Q. C. (2018). Adaptive introgression: a plant perspective. *Biology*
828 *letters*, 14(3), 20170688.

829 Taylor, S., & Larson, E. (2019). Insights from genomes into the evolutionary importance and prevalence of
830 hybridization in nature. *Nature Ecology & Evolution*, 3, 170–177. [https://doi.org/10.1038/s41559-018-](https://doi.org/10.1038/s41559-018-0777-y)
831 [0777-y](https://doi.org/10.1038/s41559-018-0777-y)

832 Toews, D. P., & Brelsford, A. (2012). The biogeography of mitochondrial and nuclear discordance in
833 animals. *Molecular Ecology*, 21(16), 3907–3930.

834 Uetz, P., Freed, P., Aguilar, R., Reyes, F., Kudera, J., & Hošek, J. (2024). The Reptile Database. Retrieved
835 2024 from <http://www.reptile-database.org>

836 Vargas, O. M., Ortiz, E. M., & Simpson, B. B. (2017). Conflicting phylogenomic signals reveal a pattern of
837 reticulate evolution in a recent high-Andean diversification (Asteraceae: Astereae: *Diplostephium*).
838 *New Phytol*, 214(4), 1736–1750. <https://doi.org/10.1111/nph.14530>

839 Vavrek, M. J. (2011). Fossil: palaeoecological and palaeogeographical analysis tools. *Palaeontologia*
840 *electronica*, 14(1), 16.

841 Wang, J. (2022). Fast and accurate population admixture inference from genotype data from a few
842 microsatellites to millions of SNPs. *Heredity*, 129(2), 79–92.

843 Weir, B. S., & Cockerham, C. C. (1984). Estimating F-statistics for the analysis of population structure.
844 *Evolution*, 1358–1370.

845 Weir, B. S., & Hill, W. G. (2002). Estimating F-statistics. *Annual review of genetics*, 36(1), 721–750.

846 Wilson, S., & Swan, G. (2020). A complete Guide to Reptiles of Australia. New Holland Publishers.

847 Wogan, G. O. U., Yuan, M. L., Mahler, D. L., & Wang, I. J. (2023). Hybridization and Transgressive Evolution
848 Generate Diversity in an Adaptive Radiation of *Anolis* Lizards. *Systematic Biology*, 72(4), 874–884.
849 <https://doi.org/10.1093/sysbio/syad026>

850 Wright, S. (1943). Isolation by distance. *Genetics*, 28(2), 114.

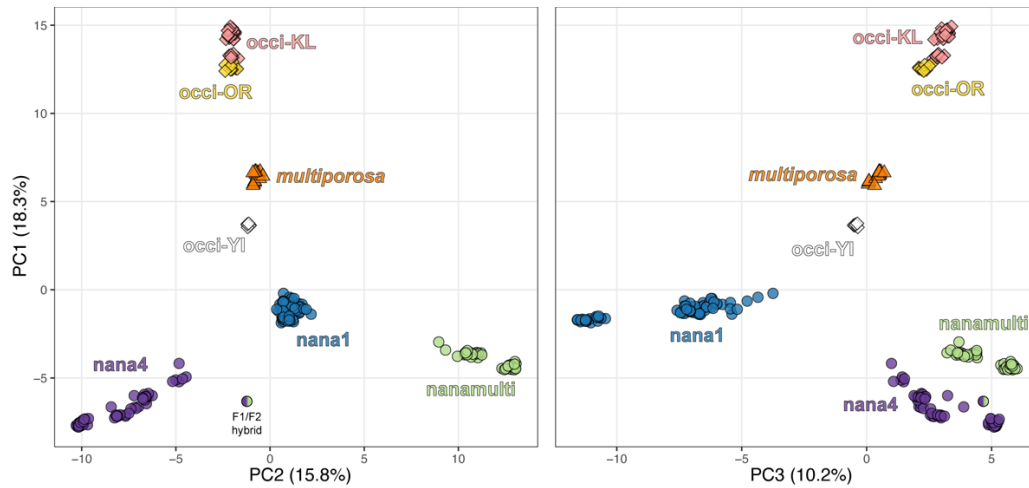
851 Zhang, D., Tang, L., Cheng, Y., Hao, Y., Xiong, Y., Song, G., Qu, Y., Rheindt, F. E., Alström, P., Jia, C., & Lei, F.
852 (2019). “Ghost Introgression” As a Cause of Deep Mitochondrial Divergence in a Bird Species Complex.
853 *Molecular Biology and Evolution*, 36(11), 2375–2386. <https://doi.org/10.1093/molbev/msz170>

854 Zieliński, P., Nadachowska-Brzyska, K., Wielstra, B., Szkotak, R., Covaciu-Marcov, S., Cogălniceanu, D., &
855 Babik, W. (2013). No evidence for nuclear introgression despite complete mt DNA replacement in the
856 Carpathian newt (*Lissotriton montandoni*). *Molecular Ecology*, 22(7), 1884–1903.

857 Zozaya, S. M., Macor, S. A., Schembri, R., Higgie, M., Hoskin, C. J., O'Hara, K., Lau, C. C., Read, W. J., &
858 Moritz, C. (2024). Contact zones reveal restricted introgression despite frequent hybridization across a
859 recent lizard radiation. *Evolution*, qpae174. <https://doi.org/10.1093/evolut/qpae174>
860

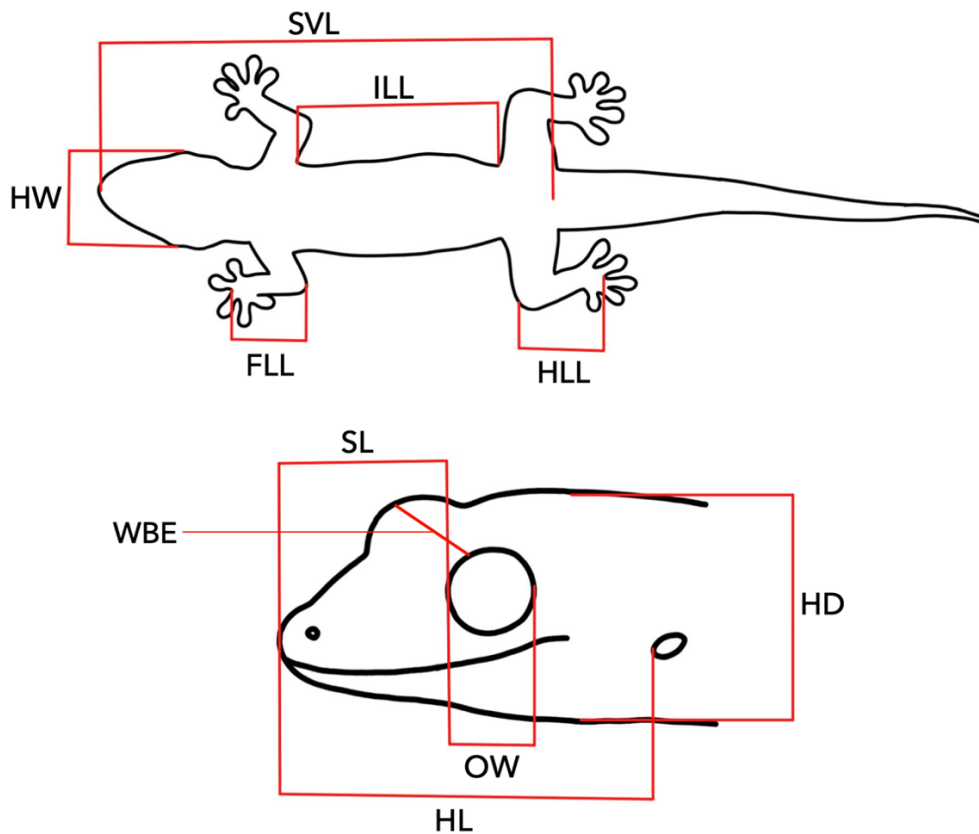
861
862

Supplementary material



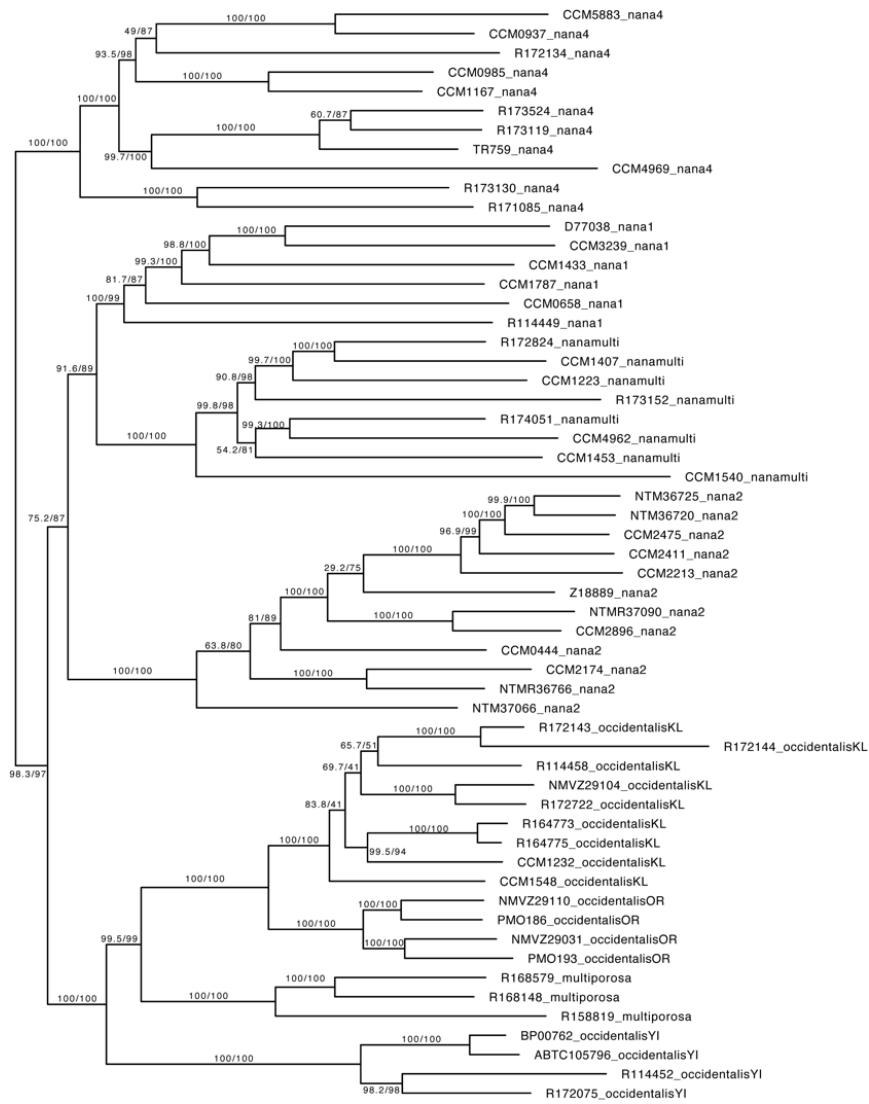
863
864
865
866
867
868

Figure S1. Ordination plots showing PC 1–3 from principal coordinates analyses (PCoA) of genome-wide SNP data across the *Gehyra nana-occidentalis* group.



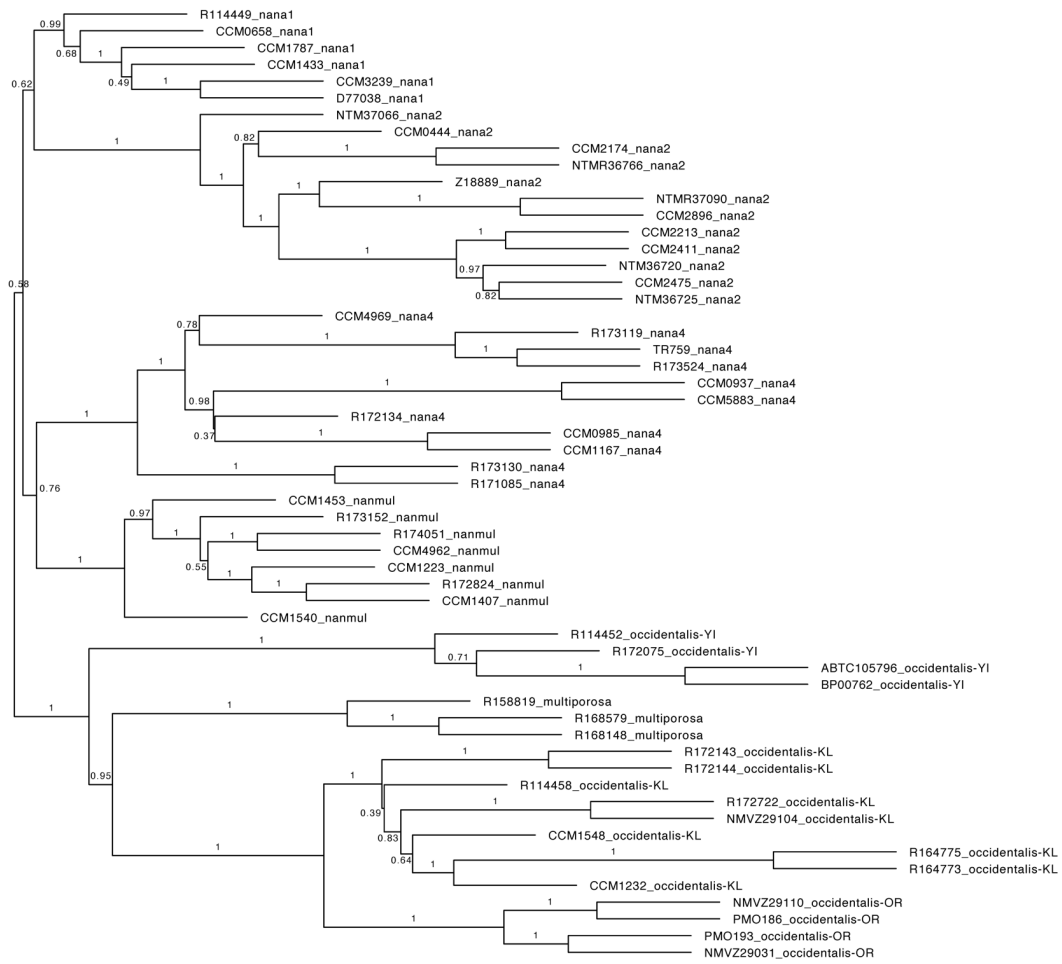
869
870
871
872

Figure S2. Morphological traits measured in this study. Traits and abbreviations are as follows: snout-to-vent length (SVL); head width (HW); inter-limb length (ILL); forelimb length (FLL); hindlimb length (HLL); snout length (SL); width-between-eyes (WBE); orbit width (OW); head depth (HD); head length (HL).



873
874
875
876
877
878
879

Figure S3. Phylogeny of the *Gehyra nana-occidentalis* group inferred from a concatenated alignment of 1,478 exons using IQ-TREE. Numbers on branches indicate SH-like aLRT / ultrafast bootstrap support.



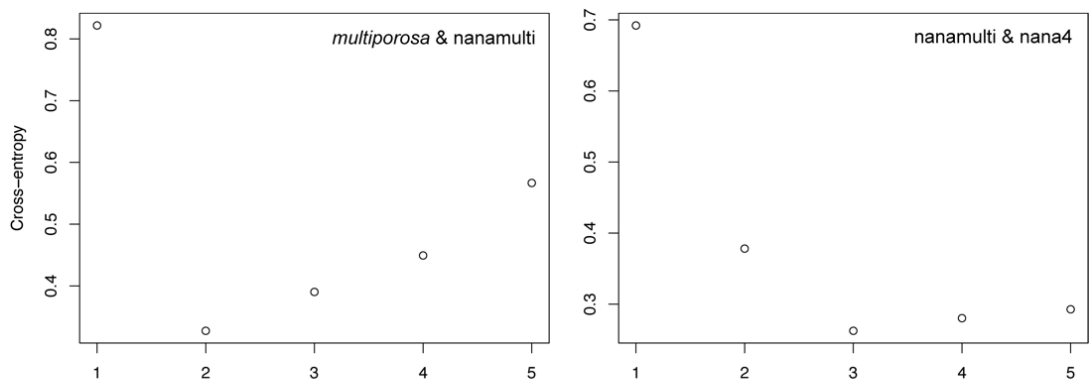
880
881
882
883
884
885
886
887

Figure S4. Phylogeny of the *Gehyra nana-occidentalis* group inferred from 1,478 gene trees using ASTRAL-III. Branches on gene trees with bootstrap support < 30 were collapsed. Numbers on branches indicate posterior probabilities.



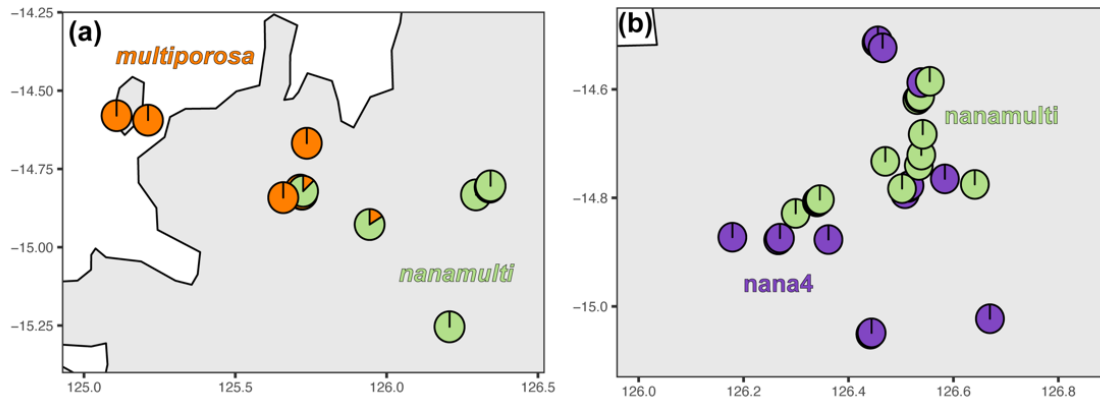
888
889
890
891
892
893
894
895

Figure S5. Mitochondrial phylogeny of the *Gehyra nana-occidentalis* group inferred from 1,038 bp of the ND2 locus using IQ-TREE. Lineages are collapsed for graphical purposes where possible.



896
897
898
899
900
901

Figure S6. Cross entropy (ce) scores from sNMF for K = 1–5 at the two contact zones.



902
903
904
905
906
907
908
909
910
911

Figure S7. Maps each show pie charts that reflect individual admixture proportions estimated by sNMF at $K = 2$ at the two contact zones.

Table S1. Exon capture samples for the *Gehyra nana-occidentalis* group used in phylogenomics and introgression analyses. All samples were used in ASTRAL-III and IQ-TREE analysis. The 'BPP phylogeny' column indicates whether the sample was use in the BPP phylogenomics analysis, and 'BPP MSCi' indicates whether the sample was used in at least one of the MSCi analyses.

Sample ID	Lineage	BPP Phylogeny	BPP MSCi	Latitude	Longitude
CCM1217	<i>multiporosa</i>	No	No	-14.8317	125.7192
R158819	<i>multiporosa</i>	Yes	Yes	-14.601944	125.203889
R168148	<i>multiporosa</i>	Yes	Yes	-15.5944	125.1872
R168579	<i>multiporosa</i>	Yes	Yes	-15.283333	124.383333
CCM0534	nana1	No	No	-15.61091	131.11597
CCM0658	nana1	Yes	No	-15.75056	129.08692
CCM1433	nana1	No	No	-17.52945	126.20999
CCM1787	nana1	Yes	No	-17.66931	128.30934
CCM3239	nana1	No	No	-18.3272	125.765
D77007	nana1	No	No	-17.14182	125.23882
D77038	nana1	Yes	No	-18.75114	126.08203
R114449	nana1	Yes	No	-16.15	123.75
CCM0444	nana2	Yes	No	-14.43816	132.28014
CCM2174	nana2	Yes	No	-14.71124	134.28859
CCM2213	nana2	No	No	-14.76098	134.68181
CCM2411	nana2	No	No	-14.65498	134.7812
CCM2475	nana2	No	No	-14.27311	135.06345
CCM2896	nana2	No	No	-13.11446	130.79838
CCM3548	nana2	No	No	-14.219667	132.040333
CCM3550	nana2	No	No	-14.219667	132.040333
NTM36720	nana2	No	No	-14.178	134.364
NTM36725	nana2	No	No	-14.089333	134.571833
NTM37066	nana2	No	No	-14.814117	131.918833
NTMR36766	nana2	No	No	-14.132833	134.343
NTMR37090	nana2	Yes	No	-13.285067	131.117433
Z18889	nana2	Yes	No	-12.188333	133.8125
CCM0937	nana4	No	No	-14.52463	126.46395
CCM0985	nana4	Yes	Yes	-14.88	126.35853
CCM1167	nana4	Yes	Yes	-14.7699	126.5788
CCM4969	nana4	No	No	-14.349779	127.750982
CCM5883	nana4	No	No	-14.595349	126.541894
R171085	nana4	No	No	-15.078056	128.141389
R172134	nana4	No	No	-13.9391	126.1744
R173119	nana4	No	No	-14.60824	126.93479
R173130	nana4	Yes	Yes	-15.81666	128.09793
R173524	nana4	No	No	-14.60824	126.93172
TR759	nana4	Yes	Yes	-15.0053	126.83661
CCM1182	nanamulti	Yes	Yes	-14.8237	125.7213
CCM1223	nanamulti	Yes	Yes	-14.8237	125.7213
CCM1407	nanamulti	No	No	-16.49599	125.3393

Sample ID	Lineage	BPP Phylogeny	BPP MSCi	Latitude	Longitude
CCM1453	nanamulti	No	No	-17.29092	127.25687
CCM1540	nanamulti	No	No	-16.81862	126.22401
CCM4962	nanamulti	Yes	No	-14.49111	127.65298
R172824	nanamulti	No	No	-16.6575	125.929167
R173152	nanamulti	Yes	Yes	-14.58944	126.55067
R174051	nanamulti	No	Yes	-14.77614	127.09767
CCM1232	occidentalis-KL	Yes	Yes	-17.04067	125.2268
CCM1548	occidentalis-KL	Yes	Yes	-16.81862	126.22401
NMVZ29104	occidentalis-KL	No	No	-17.48246	125.02902
R114458	occidentalis-KL	No	No	-16.083333	123.416667
R146018	occidentalis-KL	No	No	-16.6833	123.8333
R164773	occidentalis-KL	No	No	-16.7452	128.2825
R164775	occidentalis-KL	Yes	Yes	-16.745278	128.2825
R172143	occidentalis-KL	No	Yes	-16.0816	124.0706
R172144	occidentalis-KL	No	No	-16.0925	124.0931
R172722	occidentalis-KL	Yes	Yes	-17.408333	124.946111
NMVZ29031	occidentalis-OR	Yes	Yes	-17.91662	125.3024
NMVZ29110	occidentalis-OR	Yes	Yes	-17.558272	125.098489
PMO186	occidentalis-OR	Yes	Yes	-17.6748	125.0704
PMO193	occidentalis-OR	Yes	Yes	-18.02674	125.54425
ABTC105796	occidentalis-YI	Yes	No	-16.429167	123.178611
BP00762	occidentalis-YI	Yes	Yes	-16.43	123.18
R114452	occidentalis-YI	Yes	Yes	-16.15	123.7833
R165445	occidentalis-YI	No	No	-16.083889	123.541944
R172075	occidentalis-YI	Yes	Yes	-16.622778	123.470833
ABTC29238	paranana	No	No	-13.73	130.73
CCM0651	paranana	No	No	-15.65862	129.65944
CCM0652	paranana	No	No	-15.65862	129.65944
CCM2881	paranana	No	No	-13.19654	130.71394
CCM2936	paranana	No	No	-13.12641	130.80463
NTM37056	paranana	No	No	-13.35	131.138

912
913
914
915
916
917

Table S2. Samples for which we obtained genome-wide SNP data via DArTseq, their respective lineage, latitude, longitude, whether they were an early generation hybrid, and the contact zone they were included in (if applicable).

Sample ID	Lineage	Latitude	Longitude	Early gen hybrid?	Contact zone
CCM1185	<i>multiporosa</i>	-14.8317	125.7192		multiporosa/nanamulti
CCM1186	<i>multiporosa</i>	-14.8317	125.7192		multiporosa/nanamulti
CCM1211	<i>multiporosa</i>	-14.6723	125.7319		multiporosa/nanamulti
CCM1215	<i>multiporosa</i>	-14.8317	125.7192		multiporosa/nanamulti
CCM1217	<i>multiporosa</i>	-14.8317	125.7192		multiporosa/nanamulti
CCM2820	<i>multiporosa</i>	-14.82168	125.70993		multiporosa/nanamulti
R168148	<i>multiporosa</i>	-15.5944	125.1872		
WAMR158819	<i>multiporosa</i>	-14.601944	125.20389		multiporosa/nanamulti
WAMR158824	<i>multiporosa</i>	-14.601944	125.20389		multiporosa/nanamulti
WAMR168575	<i>multiporosa</i>	-15.35	124.53333		
WAMR168576	<i>multiporosa</i>	-15.35	124.53333		
WAMR168579	<i>multiporosa</i>	-15.283333	124.38333		
WAMR168585	<i>multiporosa</i>	-15.351	125.001		
WAMR168905	<i>multiporosa</i>	-14.585556	125.10222		multiporosa/nanamulti
WAMR171078	<i>multiporosa</i>	-15.026944	124.95389		
ABTC118947	nana1	-16.634715	129.33521		
CCM0534	nana1	-15.61091	131.11597		
CCM0658	nana1	-15.75056	129.08692		
CCM1433	nana1	-17.52945	126.20999		
CCM1489	nana1	-17.13767	125.07829		
CCM1787	nana1	-17.66931	128.30934		
CCM1803	nana1	-17.64743	127.69274		
CCM2716	nana1	-15.645	130.4959		
CCM2720	nana1	-15.9354	129.6105		
CCM2723	nana1	-15.7652	128.7402		

Sample ID	Lineage	Latitude	Longitude	Early gen hybrid?	Contact zone
CCM2808	nana1	-16.11707	128.73813		
CCM2951	nana1	-15.87227	130.32527		
CCM2984	nana1	-16.45158	130.10257		
CCM2998	nana1	-16.31998	130.44366		
CCM3015	nana1	-17.51892	129.87592		
CCM3033	nana1	-18.42522	127.81967		
CCM3079	nana1	-16.74565	128.28288		
CCM3095	nana1	-17.33473	128.38443		
CCM3239	nana1	-18.3272	125.765		
CCM3427	nana1	-15.76313	128.75131		
CCM5416	nana1	-16.8	130.26667		
CCM7265	nana1	-16.57263	128.33977		
CCM7283	nana1	-16.66349	128.52646		
CCM7305	nana1	-16.7632	128.27444		
CCM7469	nana1	-16.60579	128.95433		
CCM7867	nana1	-15.6586	129.659		
CCM7868	nana1	-15.6586	129.659		
CCM8043	nana1	-17.9025	127.8313		
CCM8044	nana1	-17.9025	127.8313		
D76950	nana1	-17.90913	125.28525		
D77007	nana1	-17.14182	125.23882		
D77035	nana1	-18.75114	126.08203		
D77042	nana1	-18.73955	125.96368		
PMO172	nana1	-17.6773	125.0889		
R37204	nana1	-15.95	131.06667		
R37597	nana1	-15.034267	129.86512		
R37691	nana1	-15.025467	130.47731		
R37720	nana1	-15.283	130.83212		
SMZ1634	nana1	-15.5519	130.9186		
SMZ1635	nana1	-15.5519	130.9186		
SMZ1644	nana1	-15.5431	130.95		
SMZ1661	nana1	-15.7487	130.6251		
SMZ1713	nana1	-15.9903	128.9711		
SMZ1761	nana1	-16.7463	128.2812		
SMZ1905	nana1	-17.9148	125.2991		
SMZ1952	nana1	-18.7366	126.0944		
SMZ1964	nana1	-17.483	128.3807		
SMZ1965	nana1	-17.483	128.3807		
SMZ1966	nana1	-17.483	128.3807		
SMZ1967	nana1	-17.483	128.3807		
SMZ2829	nana1	-15.7941	128.69		
SMZ2830	nana1	-15.7941	128.69		
SMZ2834	nana1	-16.1231	128.7375		
SMZ2839	nana1	-16.0363	128.8182		
SMZ2841	nana1	-15.9833	128.9463		
SMZ2845	nana1	-16.2268	128.3442		
SMZ2847	nana1	-16.1831	128.3805		
SMZ2855	nana1	-15.8575	128.8017		
SMZ2856	nana1	-15.8575	128.8017		
SMZ2857	nana1	-15.5148	128.835		
SMZ2859	nana1	-15.7314	128.7399		
SMZ2872	nana1	-16.5734	128.1992		
SMZ2886	nana1	-15.8721	129.0511		
SMZ2917	nana1	-15.5996	131.208		
SMZ2922	nana1	-15.6057	131.0795		
SMZ3019	nana1	-17.5045	126.1106		
SMZ3038	nana1	-17.5297	126.2131		
WAMR114449	nana1	-16.15	123.75		
ABTC112801	nana4	-13.939167	126.17444		
BP02484	nana4	-14.486407	127.81917		
CCM0727	nana4	-15.1998	126.0874		multiporosa/nanamulti
CCM0921	nana4	-14.52463	126.46395		nana4/nanamulti
CCM0986	nana4	-14.88	126.35853		multiporosa/nanamulti
CCM1167	nana4	-14.7699	126.5788		nana4/nanamulti

Sample ID	Lineage	Latitude	Longitude	Early gen hybrid?	Contact zone
CCM1665	nana4	-15.72028	127.81917		
CCM1751	nana4	-14.8791	126.172		multiporosa/nanamulti
CCM4968	nana4	-14.349779	127.75098		
CCM4971	nana4	-14.79563	127.93694		
CCM5883	nana4	-14.595349	126.54189		nana4/nanamulti
CCM7444	nana4	-15.53519	128.71225		
CCM7448	nana4	-15.17884	128.63002		
CCM7964	nana4	-14.7826	126.5112		nana4/nanamulti
CCM7965	nana4	-14.782806	126.51103		nana4/nanamulti
CCM7966	nana4	-14.782806	126.51103		nana4/nanamulti
CCM7967	nana4	-14.7826	126.5112		nana4/nanamulti
CCM7968	nana4	-14.7826	126.5112		nana4/nanamulti
CCM8005	nana4	-14.5885	126.5376		nana4/nanamulti
CCM8053	nana4	-15.8039	128.5048		
CCM8054	nana4	-15.8039	128.5048		
CMWA69	nana4	-15.90715	128.12544		
R173130	nana4	-15.81666	128.09793		
R174186	nana4	-14.5178	126.4489		nana4/nanamulti
R174189	nana4	-14.51675	126.45035		nana4/nanamulti
SMZ1501	nana4	-15.803	128.5066		
SMZ1723	nana4	-15.7144	128.2555		
SMZ1724	nana4	-15.7144	128.2555		
SMZ1725	nana4	-15.86455	128.38844		
SMZ1726	nana4	-15.864262	128.38949		
SMZ1763	nana4	-15.9698	128.4202		
SMZ1772	nana4	-15.782875	128.55258		
SMZ1773	nana4	-15.770748	128.6183		
SMZ1774	nana4	-15.7707	128.6183		
SMZ1776	nana4	-15.770217	128.61919		
SMZ1796	nana4	-14.881707	126.26184		multiporosa/nanamulti
SMZ1797	nana4	-14.8817	126.2618		multiporosa/nanamulti
SMZ1798	nana4	-14.8817	126.2618		multiporosa/nanamulti
SMZ1820	nana4	-14.5884	126.5375		nana4/nanamulti
SMZ1821	nana4	-14.5884	126.5375		nana4/nanamulti
SMZ1822	nana4	-14.5884	126.5375		nana4/nanamulti
SMZ1823	nana4	-14.5884	126.5375		nana4/nanamulti
SMZ1877	nana4	-14.783062	126.51078		nana4/nanamulti
SMZ1878	nana4	-14.782762	126.51114		nana4/nanamulti
SMZ1879	nana4	-14.7837	126.5098		nana4/nanamulti
SMZ2828	nana4	-15.7871	128.6792		
SMZ2843	nana4	-16.3598	128.225		
SMZ2849	nana4	-16.1113	128.3818		
SMZ2851	nana4	-16.0617	128.4062		
SMZ2884	nana4	-15.7674	128.6523		
SMZ3000	nana4	-16.0143	128.0137		
SMZ3006	nana4	-16.0127	127.9768		
TR758	nana4	-15.01073	126.83552	nanamulti/nana4	
TS1614	nana4	-15.056383	126.43642		multiporosa/nanamulti
TS1615	nana4	-15.056383	126.43642		multiporosa/nanamulti
WAMR172336	nana4	-14.8	126.5		nana4/nanamulti
WAMR172912	nana4	-15.1324	126.1474		multiporosa/nanamulti
WAMR173119	nana4	-14.60824	126.93479		
WAMR174107	nana4	-15.02725	126.66505		
ABTC137453	nanamulti	-16.44338	127.78315		
BPO2238	nanamulti	-14.740131	128.30336		
CCM0764	nanamulti	-15.3522	126.5899		
CCM0880	nanamulti	-14.83431	126.29359		multiporosa/nanamulti
CCM1017	nanamulti	-16.0969	126.5112		
CCM1065	nanamulti	-15.2609	126.201		multiporosa/nanamulti
CCM1160	nanamulti	-14.7811	126.6349		nana4/nanamulti
CCM1223	nanamulti	-14.8237	125.7213		multiporosa/nanamulti
CCM1407	nanamulti	-16.49599	125.3393		
CCM1453	nanamulti	-17.29092	127.25687		
CCM1501	nanamulti	-16.90368	125.7606		

Sample ID	Lineage	Latitude	Longitude	Early gen hybrid?	Contact zone
CCM1538	nanamulti	-16.81862	126.22401		
CCM1546	nanamulti	-16.81862	126.22401		
CCM1571	nanamulti	-16.53559	126.12857		
CCM1573	nanamulti	-16.53559	126.12857		
CCM1600	nanamulti	-16.49046	126.21177		
CCM1626	nanamulti	-16.17108	125.98763		
CCM4962	nanamulti	-14.49111	127.65298		
CCM7969	nanamulti	-14.7892	126.4957		nana4/nanamulti
CCM8004	nanamulti	-14.5947	126.5438		nana4/nanamulti
CCM8041	nanamulti	-15.9377	127.2216		
CCM8042	nanamulti	-15.9377	127.2216		
MCZA28615	nanamulti	-14.58944	126.55067		nana4/nanamulti
R172825	nanamulti	-16.6575	125.92917		
R174051	nanamulti	-14.77614	127.09767		
SMZ1499	nanamulti	-14.9336	125.9376		multiporosa/nanamulti
SMZ1807	nanamulti	-14.811018	126.33762		multiporosa/nanamulti
SMZ1808	nanamulti	-14.810548	126.3367		multiporosa/nanamulti
SMZ1809	nanamulti	-14.811297	126.33703		multiporosa/nanamulti
SMZ1810	nanamulti	-14.811301	126.3371		multiporosa/nanamulti
SMZ1837	nanamulti	-14.594393	126.54423		nana4/nanamulti
SMZ1838	nanamulti	-14.59335	126.54457		nana4/nanamulti
SMZ1839	nanamulti	-14.593392	126.54453		nana4/nanamulti
SMZ1840	nanamulti	-14.594937	126.54378		nana4/nanamulti
SMZ1847	nanamulti	-14.619821	126.52953		nana4/nanamulti
SMZ1848	nanamulti	-14.620619	126.52931		nana4/nanamulti
SMZ1849	nanamulti	-14.6206	126.5293		nana4/nanamulti
SMZ1855	nanamulti	-14.690829	126.53347		nana4/nanamulti
SMZ1858	nanamulti	-14.723562	126.5363		nana4/nanamulti
SMZ1860	nanamulti	-14.743422	126.53065		nana4/nanamulti
TS1606	nanamulti	-14.73675	126.4661		nana4/nanamulti
WAMR172831	nanamulti	-15.957778	127.0625		
CCM1293	occidentalis-KL	-16.78657	124.92196		
CCM1303	occidentalis-KL	-16.97111	125.02998		
CCM1337	occidentalis-KL	-17.11856	125.13182		
CCM1374	occidentalis-KL	-16.49954	125.33637		
CCM1439	occidentalis-KL	-17.52933	126.21127		
CCM1493	occidentalis-KL	-17.16653	125.34761		
CCM1548	occidentalis-KL	-16.81862	126.22401		
CCM1566	occidentalis-KL	-16.53559	126.12857		
CCM1670	occidentalis-KL	-16.34058	126.24382		
CCM7366	occidentalis-KL	-17.17496	125.29897		
CCM7625	occidentalis-KL	-16.74726	128.28123		
CCM7628	occidentalis-KL	-16.74726	128.28123		
CCM7630	occidentalis-KL	-16.74726	128.28123		
CCM8073	occidentalis-KL	-16.6558	125.9256		
CCM8074	occidentalis-KL	-16.6558	125.9256		
CCM8075	occidentalis-KL	-16.6558	125.9256		
PMO174	occidentalis-KL	-17.47945	125.02886		
R172143	occidentalis-KL	-16.0816	124.0706		
R172144	occidentalis-KL	-16.0925	124.0931		
R172724	occidentalis-KL	-17.408333	124.94611		
R172731	occidentalis-KL	-17.432222	124.98083		
R172797	occidentalis-KL	-17.432222	124.98083		
R172798	occidentalis-KL	-17.34001	124.8242		
SMZ3016	occidentalis-KL	-17.5045	126.1106		
SMZ3020	occidentalis-KL	-17.5293	126.2121		
WAMR171593	occidentalis-KL	-15.976944	125.36667		
CCM3311	occidentalis-OR	-18.1048	125.6919		
D76949	occidentalis-OR	-17.90913	125.28525		
PMO181	occidentalis-OR	-17.69499	125.14423		
PMO186	occidentalis-OR	-17.6748	125.0704		
PMO203	occidentalis-OR	-18.1064	125.6899		
PMO207	occidentalis-OR	-18.02732	125.54452		
PMO212	occidentalis-OR	-18.0272	125.54402		

Sample ID	Lineage	Latitude	Longitude	Early gen hybrid?	Contact zone
R172720	occidentalis-OR	-17.607778	125.14556		
SMZ3281	occidentalis-OR	-17.9149	125.2998		
WAMR172719	occidentalis-OR	-17.607778	125.14556		
R146018	occidentalis-YI	-16.6833	123.8333		
R165445	occidentalis-YI	-16.083889	123.54194		
R165551	occidentalis-YI	-16.141111	123.74861		
R168303	occidentalis-YI	-16.020119	123.51924		
R172076	occidentalis-YI	-16.254167	123.82444		
R172097	occidentalis-YI	-16.6225	123.47139		
CCM7831	<i>paranana</i>	-13.12576	130.80212		
CCM7832	<i>paranana</i>	-13.12576	130.80212		
CCM7834	<i>paranana</i>	-13.12576	130.80212		
CCM7836	<i>paranana</i>	-13.12576	130.80212		
CCM7864	<i>paranana</i>	-15.6586	129.659		
CCM7865	<i>paranana</i>	-15.6586	129.659		
CCM7866	<i>paranana</i>	-15.6586	129.659		
CDU375	<i>paranana</i>	-13.12468	130.7995		
CDU376	<i>paranana</i>	-13.12468	130.7995		
CDU378	<i>paranana</i>	-13.12468	130.7995		
CDU380	<i>paranana</i>	-13.12468	130.7995		
CDU546	<i>paranana</i>	-13.20427	130.7139		
R37601	<i>paranana</i>	-15.034267	129.86512		
SMZ2025	<i>paranana</i>	-13.2179	130.7355		
SMZ2026	<i>paranana</i>	-13.2179	130.7355		
SMZ2027	<i>paranana</i>	-13.2179	130.7355		

918

919

Table S3. Information for the four contact zones examined herein.

Lineage 1	Lineage 2	Variant sites	Latitude	Longitude	Radius
nanamulti	nana4	2,192	-14.80102	126.48523	40 km
<i>multiporosa</i>	nanamulti	1,828	-14.95255	125.74066	80 km

920

921

922

923

924

925

926

Table S4. Samples used in analyses of morphological data. Sample ID numbers all represent WAM R accession numbers. Columns 4–13 represent linear morphometric variables in mm, abbreviations for which are as follows: SVL, snout-to-vent length; HL, head length; HD, head depth; HW, head width; SL, snout length; OW, orbit width; WBE, width-between-eyes; ILL, interlimb length; HLL, hindlimb length; FLL, forelimb length.

Sample ID	Sex	Lineage	SVL	HL	HD	HW	SL	OW	WBE	ILL	HLL	FLL
167804	m	<i>multiporosa</i>	49.99	11.58	5.5	9.75	5.11	3.53	3.54	21.44	7.33	6.24
171491	m	<i>multiporosa</i>	53.24	12.58	5.76	10.6	5.53	3.82	3.77	22.91	7.4	6.3
168577	m	<i>multiporosa</i>	52.15	12.35	5.24	10.12	5.1	3.55	3.7	21.39	7.19	6.45
168584	f	<i>multiporosa</i>	53.77	12.38	5.48	10.27	5.5	3.81	3.94	22.69	7.23	6.4
168177	f	<i>multiporosa</i>	55.28	12.85	5.49	10.13	5.62	3.77	3.9	24.28	7.19	6.63
171547	f	<i>multiporosa</i>	47.46	11.88	4.7	9.59	5.06	3.48	3.57	20.45	7.01	6.16
168902	f	<i>multiporosa</i>	50.71	11.85	5.29	9.4	5.2	3.71	3.22	22.18	7.58	6.16
167855	m	<i>multiporosa</i>	48.98	11.83	5.39	9.39	5.13	3.52	3.23	21.75	7.58	6.57
96949	f	<i>multiporosa</i>	53.8	12.48	5.07	10.29	5.27	4.24	3.71	23.24	7.9	6.69
172066	m	<i>multiporosa</i>	51.98	12.32	5.49	10.15	5.21	4.12	3.64	23.66	7.26	6.31
168587	m	<i>multiporosa</i>	50.83	12.34	5.22	10.28	5.22	3.93	3.37	22.99	7.12	6.13
168711	f	<i>multiporosa</i>	53.45	12.45	5.19	10.23	5.49	4.03	3.25	23.28	7.2	6.35
158819	f	<i>multiporosa</i>	45.66	11.25	4.98	9.14	4.9	3.51	3.03	20.74	6.14	5.44
168582	m	<i>multiporosa</i>	50.52	12.34	4.96	9.31	5.28	3.49	3.05	22.6	7.04	5.95
168732	f	<i>multiporosa</i>	49.84	11.67	4.81	9.96	5.05	3.43	2.94	22.4	6.62	6.25
83711	m	occidentalis-KL	57.94	13.94	6.51	10.98	6.11	3.84	3.75	25.82	8.65	7.6
176207	f	occidentalis-KL	41.73	10.99	4.22	8.6	4.6	3.53	2.82	18.27	5.81	5.34
175756	m	occidentalis-KL	66.6	16.02	7.14	12.56	6.99	4.63	4.74	29.71	10.04	9.02
175752	m	occidentalis-KL	63.44	14.84	5.88	12.21	6.16	4.36	4.31	28.9	9.32	8.67
175764	f	occidentalis-KL	49.77	12.24	4.65	9.37	4.97	3.69	3.22	23.85	6.65	6.33
175760	m	occidentalis-KL	61.44	14.58	6.14	11.21	6.16	4.24	4.27	28.24	8.84	7.78
175755	m	occidentalis-KL	59.62	14.25	5.88	10.93	6.03	4.27	4.05	27.32	8.67	7.88
175761	f	occidentalis-KL	60.76	15.76	6.42	12.42	6.68	4.57	4.4	25.63	8.99	8.3
175753	f	occidentalis-KL	54.11	13.96	5.03	10.77	5.64	4.14	3.82	23.42	8.05	7.13
175757	m	occidentalis-KL	64.26	15.37	6.78	12.13	6.4	4.21	4.45	28.74	9.2	8.63
175762	f	occidentalis-KL	60.9	15.2	5.98	11.71	6.28	4.55	4.1	27.49	8.84	8.1

Sample ID	Sex	Lineage	SVL	HL	HD	HW	SL	OW	WBE	ILL	HLL	FLL
175490	f	occidentalis-KL	60.11	14.06	5.39	11.57	6.4	4.58	4.04	26.44	9.13	8.11
172798	f	occidentalis-KL	56.68	14.55	6.13	11.07	6.16	4.43	4.07	25.13	9.21	8.29
175758	f	occidentalis-KL	55.58	13.47	5.26	10.69	5.69	4.1	3.99	24.4	8.4	7.35
172768	m	occidentalis-KL	62.54	14.89	6.6	11.35	6.36	4.66	4.26	28.13	9.83	8.35
172826	f	occidentalis-KL	60.56	14.55	5.55	11.24	6.12	4.36	4.19	28.6	8.71	7.68
175482	m	occidentalis-KL	63.67	15.48	6.22	12.34	6.29	4.95	4.6	28.76	9.8	8.84
172778	f	occidentalis-KL	63.1	15.25	6.49	11.74	6.49	4.53	4.31	28.61	9.38	8.22
175479	m	occidentalis-KL	65.81	15.75	6.7	12.53	6.65	4.74	4.63	28.49	9.88	8.91
172786	m	occidentalis-KL	57.39	14.53	6.11	11.62	6.26	4.49	4.26	25.54	8.76	8.19
175488	f	occidentalis-KL	58.56	14.53	5.31	11.69	6.16	4.45	4.36	24.13	9.08	8.22
175481	f	occidentalis-KL	59.63	14.3	6.58	11.96	6.22	4.32	4.26	26.84	9.33	8.39
175497	f	occidentalis-KL	56.5	13.77	5.68	10.97	5.82	4.22	4.12	24.47	8.89	7.64
172785	f	occidentalis-KL	65.45	15.8	6.62	12.98	6.47	4.58	4.33	29.66	9.23	8.54
175483	m	occidentalis-KL	62	15.5	6.03	12.33	6.25	4.37	4.16	26.18	9.07	8.39
175494	f	occidentalis-KL	62.48	15.01	6.75	11.8	6.32	4.76	4.21	28.12	9.65	9.05
175491	m	occidentalis-KL	63.63	15.32	6.86	12.12	6.47	4.51	4.24	27.06	9.57	8.67
175498	m	occidentalis-KL	53.86	13.08	5.24	10.29	5.46	3.88	3.85	23.23	8.37	7.51
175499	f	occidentalis-KL	62.14	14.56	5.84	11.61	6.3	4.2	4.21	28.57	9.27	8.4
172797	f	occidentalis-KL	65.37	15.92	6.64	12.29	6.67	4.71	4.3	29.69	9.89	8.82
172799	m	occidentalis-KL	64.05	14.93	6.23	11.72	6.48	4.47	4.4	27.84	9.77	8.83
175487	f	occidentalis-KL	47.18	12.01	4.37	8.94	5.2	4	3.45	20.54	6.69	6.43
172732	m	occidentalis-KL	65.4	16.19	6.96	12.79	6.85	4.93	4.59	28.98	10.07	9.58
172722	f	occidentalis-KL	64.51	15.97	6.56	12.64	6.67	4.78	4.39	28.74	10.25	9.1
172724	f	occidentalis-KL	58.86	15.52	6.65	11.71	6.32	4.52	4.24	26.97	9.53	9.11
172731	f	occidentalis-KL	59.26	14.89	6.11	11.26	6.16	4.8	3.91	28.37	9.3	8.6
172730	f	occidentalis-KL	64.6	16.01	7.08	12.05	6.79	4.84	4.3	28.08	9.78	9.13
172723	f	occidentalis-KL	59.08	14.71	6	11.15	6.32	4.46	4.14	26.02	9.23	8.48
172101	f	occidentalis-KL	60.52	15.32	6.64	11.94	6.3	4.76	4.38	26.94	9.63	8.79
172094	m	occidentalis-KL	62.66	15.31	6.34	11.81	6.51	4.68	4.44	28.63	8.89	8.3
172073	m	occidentalis-KL	57.18	14	6.6	11	5.83	4.33	4.18	26.53	8.53	7.32
168194	f	occidentalis-KL	60.6	14.33	5.91	11.05	6.23	5.05	4.34	26.35	8.81	8.38
164775	f	occidentalis-KL	75.13	17.96	7.52	12.97	7.78	5.42	4.73	33.88	11.93	10.78
164774	f	occidentalis-KL	66.79	16.9	6.86	12.72	7.17	4.91	4.54	29.32	10.84	10
164773	f	occidentalis-KL	62.73	15.43	6.34	11.59	6.57	4.59	4.31	28	9.8	9.02
172728	f	occidentalis-OR	55.97	13.88	6.13	10.39	5.9	4.29	3.93	25.09	8.93	8.13
172719	m	occidentalis-OR	60.87	14.99	6.32	11.29	6.17	4.68	4.18	27.02	9.3	8.36
172718	f	occidentalis-OR	56.56	13.28	5.75	10.56	5.22	4.21	3.77	24.28	8.29	7.19
172077	f	occidentalis-OR	54.53	13.76	5.57	9.64	5.67	4.3	3.72	23.38	8.33	7.71
172074	f	occidentalis-OR	63.17	15.39	6.39	11.74	6.7	4.44	4.21	27.71	9.69	8.83
172076	m	occidentalis-YI	63.22	15.57	7.11	13.03	6.46	4.7	4.56	28.54	8.73	7.81
172097	f	occidentalis-YI	55.65	13.98	6.01	10.57	5.85	4.27	4.15	25.38	7.85	6.98
172086	f	occidentalis-YI	60.09	14.96	6.52	12.29	6.33	5.07	4.46	27.61	8.69	7.85
172075	f	occidentalis-YI	61.08	14.73	6.4	11.62	6.14	4.8	4.3	28.53	8.51	7.57
165445	f	occidentalis-YI	56.92	13.73	4.76	11.29	5.89	4.32	4.15	25.12	8.09	7.27
172104	m	occidentalis-YI	54.68	13.3	5.69	10.1	5.68	4.2	4.01	25.17	7.83	7.03
172708	m	occidentalis-YI	68.96	16.32	6.58	13.1	6.96	5.14	4.93	28.24	9.29	8.2
172078	m	occidentalis-YI	60.27	14.56	6.86	11.61	5.99	4.81	4.47	26.43	8.38	7.59
158009	f	occidentalis-YI	59.07	14.03	6.89	10.88	6.03	4.25	4.36	26.62	8.27	7.43
114453	f	occidentalis-YI	57.65	14.65	6.14	10.92	6.08	4.33	4.21	24.22	7.99	7.13
168249	f	occidentalis-YI	59.76	14.65	6.35	11.49	6.2	4.58	4.29	24.89	7.97	7.31
172100	m	occidentalis-YI	58.71	14.44	6.37	10.44	6.3	4.35	4.16	25.73	7.93	7.15
172082	f	occidentalis-YI	60.42	13.88	5.87	10.66	5.99	4.29	4.08	27.22	8.09	7.42
176248	m	nanamulti	47.1	12	4.79	9.04	5.07	3.52	3.5	20.33	6.8	5.9
176439	m	nanamulti	50.99	12.37	4.99	9.99	5.47	3.7	3.68	20.7	6.9	6.39
176446	f	nanamulti	44.18	10.92	4.28	8.58	4.56	3.3	3.4	19.58	5.9	5.62
176437	f	nanamulti	45.96	10.93	4.49	9.04	4.54	3.39	3.31	19.09	5.97	5.18
176444	f	nanamulti	44.21	10.56	3.72	8.19	4.5	3.18	3.26	17.7	5.98	5.87
176280	f	nanamulti	42.76	10.71	3.62	8.41	4.38	3.09	3.33	18.7	6.29	5.61
176438	f	nanamulti	40.67	10.41	3.96	8.66	4.2	3.37	3.2	16.73	6.05	5.12
176443	f	nanamulti	43.11	11.51	4.27	8.97	4.51	3.45	3.24	19.7	6.28	5.42
176442	f	nanamulti	44.49	10.89	3.87	9.36	4.56	3.32	3.35	18.42	6.35	5.26
176450	m	nanamulti	38.89	9.71	3.88	7.4	3.78	2.95	2.92	17.89	5.8	5
176268	m	nanamulti	46.21	11.66	4.62	9.49	4.86	3.6	3.42	19.6	6.56	5.36
176433	m	nanamulti	39.74	9.94	4.09	7.89	4.07	3.19	3.13	16.61	5.72	4.97
176434	m	nanamulti	43.86	10.82	4.68	8.4	4.32	3.45	3.24	19.67	6.4	5.66
176432	f	nanamulti	41.43	10.43	4	8.65	4.38	3.11	3.16	16.78	5.82	5.02
176441	m	nanamulti	44.07	11.01	4.62	8.37	4.55	3.46	3.22	18.21	6.39	5.56
176451	m	nanamulti	42.65	10.53	4.19	8.56	4.33	3.45	3.1	18.23	6.28	5.38
176454	m	nanamulti	37.65	9.76	3.87	7.32	3.97	2.89	2.8	15.89	5.6	4.78
176448	f	nanamulti	37.45	9.53	3.47	7.76	3.89	2.74	2.71	16.56	5.45	4.65
176453	f	nanamulti	39.6	10.46	4.35	7.72	4.28	3.32	2.94	15.87	5.93	5.21

Sample ID	Sex	Lineage	SVL	HL	HD	HW	SL	OW	WBE	ILL	HLL	FLL
176330	f	nanamulti	43.42	10.81	4.48	7.37	4.34	3.4	3.14	18.04	6.33	5.9
176198	f	nanamulti	42.51	10.35	3.86	7.73	4.32	3.61	3.06	18.8	5.91	5.04
176447	m	nanamulti	46.7	11.16	4.7	8.6	4.76	3.73	3.37	21.94	6.42	5.77
176452	f	nanamulti	35.14	8.93	3.69	7.01	3.73	2.7	2.83	14.6	5.05	4.54
174207	f	nanamulti	41.97	10.67	4.95	8.21	4.33	3.14	3.03	17.76	6.3	5.42
174051	f	nanamulti	39.1	9.39	3.39	7.8	4.04	3.09	2.86	16.71	5.89	5.01
174050	f	nanamulti	43.47	10.69	4.62	8.52	4.5	3.38	3.21	19.86	6.62	5.7
172830	m	nanamulti	41.65	10.76	3.95	8.03	4.49	3.19	3.13	17.73	5.87	5.21
173150	m	nanamulti	38.49	9.17	4.12	7.06	3.95	2.96	3.02	16.86	5.74	5.09
173147	f	nanamulti	39.13	9.52	4.04	7.31	3.92	3.06	2.99	16.54	5.66	5.01
173152	m	nanamulti	38.99	9.92	4.54	7.83	4.13	3.2	2.91	15.96	5.78	5.28
172831	m	nanamulti	43.69	11.09	4.23	8.39	4.68	3.45	3.29	17.56	6.01	5.28
172824	f	nanamulti	41.77	10.23	4.28	8.18	4.37	3.42	3.12	17	6.18	5.47
172825	f	nanamulti	45.53	11.21	4.6	8.98	4.83	3.38	3.36	18.8	6.69	5.58
172832	m	nanamulti	41.53	10.52	4.09	7.59	4.29	3.24	3.1	17.3	6.06	5.37
173146	m	nanamulti	40.56	9.54	4.15	7.66	4.04	3.13	3.05	17.33	5.64	5.1
172875	f	nanamulti	39.55	9.89	3.89	7.41	4.15	3.4	2.97	16	5.85	5.2
113968	m	nanamulti	41.31	10.49	4.2	8.06	4.16	3.09	3.08	16.43	5.81	5.01
28214	m	nana4	48.65	12.25	5.68	9.89	5.26	3.4	3.26	22.03	7.89	7.02
179820	f	nana4	55.99	14.58	5.59	11.2	6.18	4.12	3.86	23.64	8.1	7.08
176164	m	nana4	47.97	12.29	4.89	9.32	5.25	3.52	3.16	20.99	7.65	6.46
176334	f	nana4	46.03	11.72	3.7	9.26	4.89	3.48	3.34	20.11	6.65	6
176187	f	nana4	38.62	9.96	3.96	7.24	4.28	3.18	3.05	15.38	5.67	4.63
176186	f	nana4	40.55	10.06	3.48	7.27	4.2	3.2	3.03	17.66	5.51	4.89
176188	f	nana4	48.59	12.36	4.84	9.45	5.28	3.95	3.42	19.83	6.9	6.18
176172	f	nana4	40.86	10.19	3.64	7.82	4.47	3.21	3.1	16.42	6.06	5.47
176199	f	nana4	50.64	12.23	4.83	8.65	5.41	3.93	3.16	21.63	6.87	6.27
176340	m	nana4	42.2	10.6	4.15	8.32	4.53	3.26	3.2	17.42	5.84	5.04
176337	m	nana4	39.97	10.04	3.92	7.67	4.23	3.1	3.17	17.28	5.86	5.14
176275	m	nana4	50.59	11.9	4.78	9.19	5.25	3.8	3.51	22.45	7.38	6.31
176333	m	nana4	44.97	11.09	4.36	8.77	4.73	3.44	3.3	20.09	6.76	5.98
176200	m	nana4	49.48	12.16	5.07	9.76	5.18	3.79	3.37	21.29	7.14	6.75
176338	f	nana4	45.31	11.43	4.76	8.18	4.69	3.57	3.54	19.66	6.53	5.51
176276	f	nana4	38.36	9.6	3.57	7.65	4.07	3.09	2.88	15.02	5.78	4.88
174107	m	nana4	46.5	11.54	4.57	8.51	5.05	3.6	3.19	21.57	6.65	6.29
174105	f	nana4	46.61	11.33	4.87	8.43	4.93	3.52	3.3	20.69	6.61	5.94
174189	m	nana4	45.58	10.89	4.47	8.56	4.67	3.45	3.42	19.1	6.36	5.73
172174	m	nana4	46.04	11.06	3.86	8.94	4.78	3.78	3.51	20.16	6.45	5.86
171086	m	nana4	47.17	11.58	4.69	8.63	4.92	3.54	3.56	20.38	6.35	5.82
171090	f	nana4	36.09	9.34	4.03	7.14	3.96	2.94	2.8	14.23	5.18	4.63
173128	m	nana4	43.15	10.9	4.73	8.49	4.54	3.49	3.24	18.21	6.19	5.58
172336	m	nana4	47.17	11.94	4.78	9.22	5.19	3.82	3.51	19.27	6.61	5.89
173524	f	nana4	39.05	9.71	3.57	7.03	4	2.93	2.96	17.06	5.7	5.19
171089	f	nana4	45.33	11.71	4.45	8.55	4.86	3.56	3.42	18.3	6.66	6.2
173129	f	nana4	42.26	10.92	4.57	8.84	4.49	3.17	3.25	17.75	6.26	5.8
172134	f	nana4	39.94	9.97	4.12	7.77	4.05	2.92	3.08	16.74	5.58	5.08
173130	m	nana4	38.22	9.86	4.13	7.56	4	3	3.03	15.29	5.76	5.29
173119	f	nana4	46.55	11.21	4.83	8.76	4.58	3.43	3.41	21.38	6.67	6.08
172135	f	nana4	39.46	10.13	4.21	7.76	4.16	3	3.07	16.19	5.76	5.42
151871	f	nana4	46.62	11.32	4.79	9.11	4.65	3.41	3.37	20.79	6.5	5.44
162518	m	nana4	47	11.67	4.65	8.59	4.81	3.36	3.17	20.57	6.69	5.89
151965	m	nana4	48.44	11.94	5.15	9.73	4.9	3.67	3.51	20.66	6.97	6.19
152015	m	nana4	49.59	11.74	5.03	9.36	4.98	3.68	3.47	21.25	7.03	6.3
151966	f	nana4	49.23	11.84	5.36	9.21	4.93	3.6	3.63	22.31	6.73	6.14
164853	m	nana4	46.72	11.54	4.64	9.25	4.97	3.47	3.37	19.94	6.38	5.79
151961	m	nana4	47.68	11.35	4.93	8.51	4.82	3.64	3.52	19.93	6.75	6.11
161187	m	nana4	45.4	11.29	5.03	8.87	4.74	3.36	3.4	19.11	6.47	6
117999	f	nana4	38.55	10.05	4.12	7.81	4.13	3.04	2.94	16.22	5.68	5.1
113991	m	nana4	39.07	10.28	4.32	7.92	4.35	3.09	3.1	15.53	5.9	5.56
117749	f	nana4	45.54	11.49	5	8.5	4.82	3.67	3.33	21.95	6.82	5.95
176223	f	nana1	42.22	10.12	3.81	7.52	4.26	3.28	3	19.57	6.15	5.69
176389	f	nana1	42.42	10.27	4.18	7.31	4.32	3.18	3.09	17.34	6.27	5.3
176301	m	nana1	39.37	9.41	3.33	7.34	4.04	3.01	2.87	16.52	5.93	5.01
175057	m	nana1	41.16	10.08	3.84	8.23	4.18	3.33	3.04	18.3	6.24	5.79
175061	m	nana1	36.56	9.46	3.74	7.31	3.88	3.02	2.78	16.4	5.78	5.14
175059	m	nana1	44.24	10.66	3.91	8.49	4.4	3.29	3.29	18.63	6.25	5.77
175053	m	nana1	42.18	10.53	4.21	8.21	4.44	3.28	3.24	18.45	6.19	5.71
175062	f	nana1	42.19	10.68	4.23	7.87	4.45	3.15	3.22	17.31	6.34	5.66
175058	m	nana1	42.16	10.07	3.56	8.37	3.98	3.11	3.24	17.32	6.17	5.73
175064	f	nana1	39.65	10	3.95	7.35	3.95	3.12	2.91	17.02	5.95	5.26
175060	m	nana1	41.14	9.91	3.72	7.66	4.08	3.27	2.89	17.07	6.08	5.62

Sample ID	Sex	Lineage	SVL	HL	HD	HW	SL	OW	WBE	ILL	HLL	FLL
175063	f	nana1	40.66	10.03	3.79	7.08	4.16	3.03	3.07	16.66	5.88	5.11
175052	f	nana1	41.06	9.7	3.78	7.49	4.14	3.15	3.02	18.41	6.09	5.56
174990	m	nana1	41.61	10.73	4.07	8.2	4.42	3.15	3.08	17.44	6.1	5.66
175050	m	nana1	37.77	9.36	3.84	7.36	3.89	2.89	2.73	16.19	5.66	4.98
132857	f	nana1	39.83	9.59	4.21	7.55	4.08	2.96	2.91	16.74	5.94	5.29
132858	f	nana1	40.42	10.07	3.9	7.6	4.3	3.22	2.96	17.38	6.07	5.34
165545	f	nana1	38.4	9.61	3.42	6.9	3.9	2.96	2.72	15.34	5.61	5.23
108735	f	nana1	40.51	9.68	3.99	7.61	4.31	2.97	2.98	18.46	5.88	5.33
125993	f	nana1	42.57	10.01	4.44	8.15	4.13	3.56	3.05	18.49	6.16	5.52
108733	m	nana1	40.27	9.8	4.2	7.6	4.11	2.99	2.94	16.25	5.7	5.22
108729	m	nana1	38.06	9.75	4.06	7.65	3.94	3	2.83	14.45	5.6	5.06

927
928
929
930
931
932
933

Table S5. Results of multivariate regression testing sexual dimorphism using RRPP. Ten log-transformed morphological traits were included as dependent variables and lineage, sex, and their interaction were included as predictor variables. Lineages included are: *occidentalis*-KL, nana4, and nana1. *P*-values < 0.05 appear in bold.

	<i>df</i>	<i>SS</i>	<i>MS</i>	<i>R</i> ²	<i>F</i>	<i>Z</i>	<i>P</i>
Lineage	2	31.861	15.9307	0.774	184.45	9.2618	0.001
Sex	1	0.252	0.2522	0.006	2.92	1.4784	0.073
Lineage*Sex	2	0.147	0.0737	0.003	0.85	0.1700	0.442
Residuals	103	8.896	0.0864	0.216			
Total	108	41.157					

934
935
936
937
938
939
940
941

Table S6. Dtrios results obtained vis *Dsuite*, with p-values adjusted using the False Discovery Rate method.

P1	P2	P3	D-statistic	Z-score	p-value (FDR)	f4-ratio
nana4	nana1	multi	0.284584	3.06836	0.0177639	0.121482
nana1	nanamulti	multi	0.0533355	0.440712	0.72783667	0.0295631
multi	occiKL	nana1	0.0695736	0.483273	0.72783667	0.0531024
multi	occiOR	nana1	0.0969976	0.684832	0.66425962	0.0913703
occiYI	multi	nana1	0.121689	0.770486	0.6389978	0.0786361
nana4	nanamulti	multi	0.282943	2.31945	0.11882733	0.147285
multi	occiKL	nana4	0.106391	0.749034	0.6389978	0.0649852
multi	occiOR	nana4	0.109319	0.824108	0.6389978	0.08476
occiYI	multi	nana4	0.0970134	0.565673	0.71452	0.0597375
occiKL	multi	nanamulti	0.145955	0.84852	0.6389978	0.054741
occiOR	multi	nanamulti	0.0648351	0.411629	0.72783667	0.0292221
occiYI	multi	nanamulti	0.466827	3.01881	0.0177639	0.151488
occiOR	occiKL	multi	0.0343869	0.247926	0.804192	0.0194288
occiKL	multi	occiYI	0.141304	0.867589	0.6389978	0.115399
occiOR	multi	occiYI	0.181241	1.05799	0.6389978	0.151047
nana4	nanamulti	nana1	0.299879	3.16211	0.0177639	0.432679
nana4	nana1	occiKL	0.275991	3.30441	0.01665591	0.154725
nana4	nana1	occiOR	0.279501	3.33162	0.01665591	0.137765
nana4	nana1	occiYI	0.242256	2.02588	0.18715025	0.127256
nanamulti	nana1	occiKL	0.100711	0.916269	0.6389978	0.0617296
nanamulti	nana1	occiOR	0.0833177	0.824518	0.6389978	0.0442314
nanamulti	nana1	occiYI	0.186203	1.58605	0.35868	0.0968816
occiKL	occiOR	nana1	0.054689	0.535398	0.71493534	0.0394492
occiYI	occiKL	nana1	0.163246	1.18426	0.59078	0.133131
occiYI	occiOR	nana1	0.167869	1.25977	0.55933231	0.164391
nana4	nanamulti	occiKL	0.180278	1.49736	0.39171125	0.0987769
nana4	nanamulti	occiOR	0.207185	1.84057	0.22989575	0.0974192
nana4	nanamulti	occiYI	0.0593474	0.403954	0.72783667	0.0338986
occiKL	occiOR	nana4	0.0326519	0.321768	0.76961809	0.0213789
occiYI	occiKL	nana4	0.13687	0.928023	0.6389978	0.124962
occiYI	occiOR	nana4	0.131131	0.840268	0.6389978	0.143437
occiKL	occiOR	nanamulti	0.0946205	0.744742	0.6389978	0.0263137
occiYI	occiKL	nanamulti	0.270576	1.92666	0.21008517	0.102762

occiYI	occiOR	nanamulti	0.277177	2.06228	0.18715025	0.125966
occiOR	occiKL	occiYI	0.0781487	0.62129	0.69275241	0.0432913

942
943
944
945
946
947
948
949
950
951
952
953
954
955

Table S7. Results of the pairwise comparison of morphometric variables across the seven lineages of the *Gehyra nana-occidentalis* group. *P*-values < 0.05 appear in bold.

Lineage pairs	<i>d</i>	UCL (95%)	Z	0.56
multiplorosa+nana1	0.671	0.368	2.641	0.001
multiplorosa+nana4	0.358	0.333	1.719	0.048
multiplorosa+nanamulti	0.548	0.335	2.433	0.001
multiplorosa+occiKL	0.629	0.325	2.686	0.001
multiplorosa+occiOR	0.515	0.575	1.414	0.105
multiplorosa+occiYI	0.559	0.417	2.060	0.014
nana1+nana4	0.320	0.297	1.715	0.048
nana1+nanamulti	0.142	0.301	0.426	0.62
nana1+occiKL	1.277	0.291	4.274	0.001
nana1+occiOR	1.156	0.551	2.903	0.001
nana1+occiYI	1.214	0.393	3.541	0.001
nana4+nanamulti	0.197	0.252	1.185	0.155
nana4+occiKL	0.966	0.241	4.092	0.001
nana4+occiOR	0.847	0.526	2.422	0.001
nana4+occiYI	0.898	0.352	3.208	0.001
nanamulti+occiKL	1.161	0.248	4.371	0.001
nanamulti+occiOR	1.042	0.532	2.769	0.001
nanamulti+occiYI	1.091	0.357	3.574	0.001
occiKL+occiOR	0.137	0.526	-0.459	0.648
occiKL+occiYI	0.152	0.356	0.309	0.449
occiOR+occiYI	0.168	0.590	-0.331	0.646

973
974
975
976
977
978
979

Table S8. Trait loadings for PC axes 1–3 for the PCA of morphological traits across the seven focal lineages of the *Gehyra nana-occidentalis* group. Values that are 70% or more of the highest loading for each axis are in bold. Abbreviations are as follows: SVL, snout-to-vent length; HL, head length; HD, head depth; HW, head width; SL, snout length; OW, orbit width; WBE, width-between-eyes; ILL, interlimb length; HLL, hindlimb length; FLL, forelimb length.

Trait (log transformed)	PC1 (95%)	PC2 (1.1%)	PC3 (0.9%)	980
SVL	-2.041	0.031	-0.026	0.981
HL	-2.039	0.014	-0.031	
HD	-1.955	-0.607	0.120	
HWL	-2.008	-0.023	-0.149	
SL	-2.031	0.011	-0.027	
OW	-1.994	0.123	-0.186	
WBE	-1.983	0.044	-0.383	
ILL	-2.007	0.034	0.078	
HLL	-2.016	0.150	0.280	
FLL	-2.003	0.207	0.321	

